NORTHWESTERN UNIVERSITY

# Harmonic Caps and Planar Conformal Geometry

A DISSERTATION

SUBMITTED TO THE GRADUATE SCHOOL

IN PARTIAL FULFILLMENT OF THE REQUIREMENTS

for the degree

DOCTOR OF PHILOSOPHY

Field of Mathematics

By

Shuyi Weng

EVANSTON, ILLINOIS

September 2020

# ABSTRACT

Harmonic Caps and Planar Conformal Geometry

Shuyi Weng

In this thesis, we study the geometry of planar shapes and their harmonic caps. Specifically, given a compact continuum $P \subseteq \mathbb{C}$, we are interested in constructing a planar cap $\hat{P}$ such that $P$ and $\hat{P}$ can be glued together along their boundary to form a topological sphere with prescribed curvature distribution. In 2017, DeMarco and Lindsey published the result that such a process is always possible if the curvature distribution is proportional to the harmonic measure associated to the complement of $P$. Alexandrov's uniqueness theorem implies that the topological sphere has a unique realization as the boundary surface of a compact convex subset of $\mathbb{R}^3$. Reshetnyak, who is one of Alexandrov's students, provided an alternative perspective of the realization from the complex analytic point of view. We build on these previous works, and characterize *harmonic planarity*, in which case said convex subset of $\mathbb{R}^3$ is entirely contained in a plane, for planar shapes that are Jordan domains or Jordan arcs. We also study computational and numerical methods for Riemann mapping constructions, including the zipper algorithm and the Schwarz-Christoffel transformations. Finally, we implement a numerical cap construction

algorithm in Mathematica and in MATLAB to generate approximations of harmonic caps. These results help us develop valuable insights into the geometric properties of harmonic caps and the associated convex realizations.

## Acknowledgements

First and foremost, I would like to express my sincere gratitude to my advisor, Laura DeMarco, without whom this thesis would never become a reality. My research greatly benefited from numerous insightful discussions with Laura. Her expertise, constant encouragement, and never-ending patience have been invaluable in the writing of this thesis. I am fortunate to have had the chance to work with such a talented mathematician and excellent mentor.

I am very grateful to the student and faculty members of the Northwestern mathematics department for their time and their friendship. Khashayar Filom, Signe Jensen, Guchuan Li, Nicole Looper, Junxiao Wang, Yuxiang Wang, and Mingyi Zhang have been particularly helpful over many insightful mathematical conversations. I want to thank Antonio Auffinger, Keith Burns, and Eric Zaslow for their guidance and attention. A special thanks to Yuxi Han, whose collaboration with Laura and me in the summer of 2017 motivated the research project that turns out to be a central topic of this thesis.

I would also like to thank my loving family for their support throughout my graduate studies from the other side of the world. Especially, I want to thank my wife, Yimei Tang, for her understanding and encouragements for my endeavors.

# Dedication

*To the memory of my loving grandmother, Yuqin Niu*

# Table of Contents

ABSTRACT 3

Acknowledgements 5

Dedication 6

Table of Contents 7

List of Figures 9

Chapter 1. Introduction 11
1.1. Summary of Main Results 14
1.2. Organization 20
1.3. Convention and Notations in this Text 20

Chapter 2. The Harmonic Measure 22
2.1. Definitions of the Harmonic Measure 22
2.2. Convergence of Harmonic Measures 24
2.3. Convergence of Conformal Metrics 26

Chapter 3. Harmonic Caps and Examples 29

Chapter 4. Harmonic Planarity of Jordan Domains 38
4.1. First Take on Jordan Domains 38
4.2. General Jordan Domains 40

Chapter 5. Harmonic Planarity of Jordan Arcs 50
5.1. Circular Arcs Are Harmonically Planar 50
5.2. Are There Other Harmonically Planar Jordan Arcs? 55

Chapter 6. Schwarz-Christoffel Transformations and the Wedge Family 60
6.1. Schwarz-Christoffel Transformations 60
6.2. The Wedge Family 65
6.3. $W_\theta$ Is Not Harmonically Planar 71

Chapter 7. Numerical Algorithms for Harmonic Cap Developments 75
7.1. Turning Angle and Curvature 75
7.2. The Cap Construction Algorithm 77

7.3. The Convex Body Associated to $W_{1/2}$ 81
7.4. The Zipper Algorithm 88

Chapter 8. Iterated Harmonic Caps and Plane Curves 92
8.1. Iterated Harmonic Caps 92
8.2. Plane Curve Iteration with the Symmetry Assumption 94

References 97

Vita 99

# List of Figures


| | | |
|---|---|---|
| 1.1 | The wedge $W_\theta$ | 18 |
| 3.1 | Harmonic cap of the unit disk | 32 |
| 3.2 | Harmonic cap of a line segment | 33 |
| 3.3 | Harmonic caps of ellipses | 34 |
| 3.4 | Convex realizations associated to ellipses | 34 |
| 3.5 | Harmonic cap of the right-angle wedge | 35 |
| 3.6 | Harmonic caps of different planar shapes | 35 |
| 3.7 | Harmonic caps of semicircular arches | 36 |
| 3.8 | Convex realizations associated to semicircular arches | 36 |
| 3.9 | Harmonic cap of the cauliflower Julia set | 37 |
| 4.1 | Convex Jordan domains have rectifiable boundary | 41 |
| 4.2 | Path integral close to the endpoint on the boundary | 44 |
| 4.3 | Alternative path integral near boundary | 45 |
| 5.1 | Symmetry condition for harmonically planar Jordan arcs | 53 |
| 5.2 | The symmetry assumption on Jordan arcs | 57 |
| 6.1 | A schematic of Schwarz-Christoffel transformations | 61 |
| 6.2 | A schematic of the conformal mapping $f\colon \mathbb{D} \to \hat{\mathbb{C}} \setminus W_\theta$ | 65 |
| 7.1 | Angular defect at identified vertex | 76 |
| 7.2 | The wedge $W_{1/2}$ and its harmonic cap | 83 |
| 7.3 | The harmonic cap of $W_{1/2}$ | 84 |
| 7.4 | Assumed caps of $W_{1/2}$ | 87 |
| 7.5 | The elementary map of the zipper algorithm | 89 |
| 7.6 | The zipper algorithm | 90 |
| 8.1 | Iterative harmonic caps of the square | 92 |
| 8.2 | The sixth iterative harmonic cap of the square | 93 |

8.3 Iterative harmonic caps of the “keyhole” and the “L” 93
8.4 The sixth iterative harmonic caps of the “keyhole” and the “L” 94
8.5 Iterative curves of the wedge family 96

CHAPTER 1

# Introduction

The purpose of this thesis is to investigate harmonic caps of planar shapes, as well as the convex bodies constructed from gluing planar shapes and their corresponding harmonic caps along the boundary. In this study, we take the perspectives of both theoretical and computational methods to further the understanding of harmonic caps.

Descartes' theorem on total angular defect states that if a polyhedron is homeomorphic to a sphere, then the sum of angular defects at the vertices is $4\pi$. We may raise the following question:

**Question.** Given a polygon $P$ in the plane, together with a prescribed distribution of angular defect on the vertices of $P$ that sums to $4\pi$, can we construct a "cap" polygon $P'$ such that $P$ and $P'$ can be glued along the boundary to form a polyhedron that is homeomorphic to a sphere?

Descartes' total angular defect theorem is a special case of Gauss-Bonnet theorem, for which the Gaussian curvature is discrete and concentrated at the vertices, and the integral of Gaussian curvature at a vertex is equal to the angular defect there [**20**]. If we think of curvature as a measure, Descartes' theorem is then the special case of Gauss-Bonnet theorem where the curvature is a discrete measure. We may raise a more general question in this setting:

**Question.** Given a Jordan domain $P$, together with a Radon measure $\mu$ supported on $\partial P$, can we construct a "cap" $P'$ such that $P$ and $P'$ can be glued along the boundary to form a topological sphere whose Gaussian curvature is proportional to $\mu$?

The answer to both questions is negative in general. For example, if a triangle is given as the polygon $P$, then the only distribution of angular defect for the "cap" polygon $P'$ to exist is that the angular defect at each vertex equals $2\pi - 2\theta$, where $\theta$ is the internal angle at the vertex. In this case, $P'$ is a reflection of $P$, and the polyhedron formed by gluing $P$ and $P'$ along the boundary is a double of the triangle $P$, thus resulting in a degenerate polyhedron. As another example, if the polygon $P$ is a quadrilateral, and the prescribed distribution of angular defect is $\pi$ at each vertex, then the "cap" polygon exists if and only if $P$ is a parallelogram. [**12**]

The study of harmonic caps begins with a version of the question that requires distribution of Gaussian curvature with respect to the harmonic measure. That is, for a fixed compact and simply connected subset $P$ of the plane, we consider the curvature distribution on $\partial P$ that is proportional to the harmonic measure for the domain $\hat{\mathbb{C}} \setminus P$ with respect to the point at $\infty$. The question, in the case of polygons and discrete curvature, dates back to the work of Alexandrov in the 1950s [**1**], but the case of curvature distribution proportional to harmonic measure has its origin in the study of complex polynomial dynamical systems. In 2017, DeMarco and Lindsey stated the question in a formal context, building on informal discussions with William Thurston and Curtis McMullen [**6**]. They provided a positive answer to the existence question of harmonic caps. We now summarize their formulation of the question, and lay out some essential definitions for the main results in this thesis.

Let $P$ be a subset of $\mathbb{C}$ or $\mathbb{R}^2$ that is compact, connected, containing at least two points, and has a connected complement. We call such subset $P$ a **planar shape**. Given a probability measure $\mu$ supported on $\partial P$, one seeks a conformal metric $\rho = \rho(z)|dz|$ on the Riemann sphere $\hat{\mathbb{C}}$ such that

(1) $P$, with Euclidean metric, embeds locally-isometrically into $(\hat{\mathbb{C}}, \rho)$; and
(2) The curvature distribution on $(\hat{\mathbb{C}}, \rho)$ equals the pushforward of $4\pi\mu$ under said embedding.

If $\rho$ exists, Alexandrov's uniqueness theorem claims that the metrized sphere $(\hat{\mathbb{C}}, \rho)$ has a unique convex realization [**1, 18**], that is, a convex subset $B \subseteq \mathbb{R}^3$ whose boundary surface is isometric to $(\hat{\mathbb{C}}, \rho)$. It is possible that $B$ does not have any interior points, or equivalently, $B$ is a two-dimensional planar region. In this case, we consider the doubling of $B$ glued along the planar boundary as the boundary surface of $B$, so that it "bounds" both sides of $B$. The complement of $P$ in $(\hat{\mathbb{C}}, \rho)$ is called the **cap** of $P$ with respect to $\mu$, and denoted by $\hat{P}_\mu$. By construction, the metric on $\hat{P}_\mu$ is flat, so it maps locally-isometrically into the standard plane $(\mathbb{C}, |dz|)$. Such a map is called a **development** of the cap $\hat{P}_\mu$. This work concerns the case where the aforementioned probability measure $\mu$ is the harmonic measure. A detailed introduction to harmonic caps of planar shapes is included in Chapter 3, where examples of numerically computed harmonic caps can also be found.

The harmonic cap problem leads us to different fields of mathematics, including computational geometry, probability, and potential theory. We have learned a number of

numerical algorithms, including the zipper algorithm [**14, 13**], Schwarz-Christoffel transformations [**9, 8, 7**], and the circle-packing algorithm [**19**] that compute numerical approximations of Riemann maps. The convex realization of Alexandrov's uniqueness theorem has also been studied by various authors, most notably Demain and O'Rouke [**5, 16**] through their study of geometric folding algorithms. The harmonic measure aspect of this problem also connects to potential theory and probability. Mörters and Peres [**15**] presented a Brownian motion's approach on potential theory in the complex plane, as well as in higher dimensions.

The central results of this thesis include two theorems concerning *harmonic planarity*, which describes the scenario that the convex realization of the metrized sphere $(\hat{\mathbb{C}}, \rho)$ can be entirely contained in a plane. A number of numerical Riemann mapping algorithms are used to find numerical approximations of the harmonic measure. Schwarz-Christoffel method is particularly useful in the in-depth study of the wedge family of planar shapes, which are Jordan arcs formed by joining two line segments of equal length at one of their endpoints. An explicit inverse distribution function of the harmonic measure is presented for the wedge family. Finally, we implement an algorithm to generate figures of harmonic caps using harmonic measure approximations generated by the numerical Riemann mapping algorithms. We call this the *cap construction algorithm*. The harmonic caps of planar shapes generated from this algorithm are included throughout this thesis.

## 1.1. Summary of Main Results

**1.1.1. Harmonic planarity.** The first point of interest is *harmonic planarity* of $P$. As a first example, if the planar shape $P$ is the closed unit disk, the harmonic measure of its

complement is uniformly distributed along the unit circle, and the associated harmonic cap $\hat{P}$ is again the unit disk. Perimeter gluing guarantees that the topological sphere formed by $P$ and its cap is a double cover of the disk itself. In this case, the convex body resulting from perimeter gluing of the unit disk and its harmonic cap is entirely contained in a plane. We say a shape is **harmonically planar** if the convex body resulting from perimeter gluing of the planar shape and its harmonic cap is entirely contained in a plane. The following theorem characterizes all Jordan domains that are harmonically planar.

**Theorem 1.1.** *Let $P \subseteq \mathbb{C}$ be the closure of a Jordan domain. Then $P$ is harmonically planar if and only if $P$ is a closed circular disk.*

If $P$ has smooth boundary, Theorem 1.1 is a relatively straightforward consequence of the boundary parameterization formula given in [**6**]. The more general case exploits the non-negativity of the curvature distribution by harmonic measure, together with a classical fact that convex Jordan domains have rectifiable boundary.

We also study planar shapes that are Jordan arcs, which are images of injective continuous functions of a bounded closed interval $[a, b]$ into the plane $\mathbb{C}$. We found a family of Jordan arcs that are harmonically planar.

**Theorem 1.2.** *If $\Gamma \subseteq \mathbb{C}$ is a line segment or a circular arc, then $\Gamma$ is harmonically planar.*

The proof of Theorem 1.2 is purely constructive, because the conformal isomorphism from the complement of the disk to the complement of a circular arc can be made explicit. We compose seven conformal maps to obtain a conformal isomorphism for any circular arc, then use such a function to construct a harmonic cap and verify its reflection symmetry.

We propose that the converse of Theorem 1.2 should also hold.

**Conjecture.** *Let $\Gamma \subseteq \mathbb{C}$ be a Jordan arc. If $\Gamma$ is harmonically planar, then it is either a line segment or a circular arc.*

Much of the work for this thesis grew out of the development of, the testing for, and various attempts to prove this conjecture. First of all, the cap construction algorithm discussed in Chapter 7, coupled with zipper algorithm [**14**] generates a family of harmonic cap examples that provide the first hints to Theorem 1.2 (see Example 3.7 and Figure 3.7). However, the implementation of zipper algorithm gives a Riemann map that fixes zero for a Jordan domain that contains zero. This requires preparation to the input data which applies a Möbius transformation that sends $\infty$ to 0 on the given planar shape and yields a bounded Jordan domain. This is not possible for Jordan arc planar shapes, because they do not have interior points. The Schwarz-Christoffel transformation discussed in Chapter 6 computes exterior Riemann maps for polygons. This algorithm overcomes previous limitation by regarding polygonal arcs as degenerate polygons without interior. It generates many harmonic cap examples of Jordan arcs, providing further evidence to the validity of the conjecture. Furthermore, the semi-explicit nature of the Schwarz-Christoffel transformation, especially the exterior map, enables us to focus on the wedge family, which are Jordan arcs formed by joining two line segments of equal length at one of their endpoints. This is the simplest non-trivial family of polygonal Jordan arcs, and we study their harmonic caps through explicit computation. Details of the wedge family will be introduced in the next subsection.

Almost every attempt to prove the conjecture deduces a *symmetry assumption* of some form. The following is one of the formulations of the *symmetry assumption*, which is a condition equivalent to being harmonically planar for a smooth Jordan arc.

**Lemma 1.3** (The Symmetry Assumption)**.** *Let $\Gamma \subseteq \mathbb{C}$ be a smooth Jordan arc, and let $\gamma\colon [0, L] \to \mathbb{C}$ be an arc-length parameterization of $\Gamma$, and assume that $\gamma(0) = 0$ and $\gamma'(0) = 1$. Let $\Phi\colon \hat{\mathbb{C}} \setminus \overline{\mathbb{D}} \to \hat{\mathbb{C}} \setminus \Gamma$ be a conformal isomorphism that fixes the point at $\infty$, and assume its continuous extension at the boundary satisfies $\Phi(1) = 0$. If $\Gamma$ is harmonically planar, then*

$$\gamma'(t) = \Phi_1^{-1}(\gamma(t)) \cdot \Phi_2^{-1}(\gamma(t)), \tag{1.1}$$

*where $\Phi_1^{-1}$ and $\Phi_2^{-1}$ are the two distinct branches of the inverse of $\Phi$ along $\Gamma$.*

Given a conformal isomorphism $\Phi$ associated with the complement of a smooth Jordan arc $\Gamma$, we can always recover the Jordan arc by the complement of the image of $\Phi$. The symmetry assumption provides yet an alternative method to recover the Jordan arc. It says that if a Jordan arc $\gamma\colon [0, L] \to \mathbb{C}$, parameterized by arc length, is harmonically planar, then the tangent vector $\gamma'(t)$ to the arc at $\gamma(t)$ equals the two preimages of $\gamma(t)$ through the conformal isomorphism $\Phi$, satisfying the conditions specified in Lemma 1.3. Invoking the fundamental theorem of calculus, the curve $\Gamma$ can be recovered up to a translation by

$$\gamma(t) = \int_0^t \Phi_1^{-1}(\gamma(x)) \cdot \Phi_2^{-1}(\gamma(x))\, dx,$$

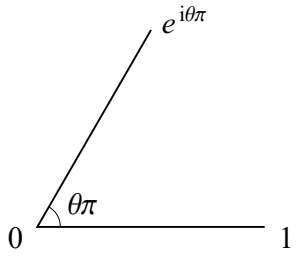


Figure 1.1. The wedge $W_\theta$

if the conformal isomorphism $\Phi$ is explicitly given. We conclude that every harmonically planar smooth Jordan arc is one with agreeing recovery from both methods. This conclusion inspires an iteration problem for smooth Jordan arcs, which is discussed in detail with numerical examples in Section 8.2.

**1.1.2. The wedge family $W_\theta$.** Schwarz-Christoffel transformation allows us to study the harmonic caps of the *wedge family* $W_\theta$ with explicit computation. This is the third family of Jordan arcs, after segments and circular arcs, whose conformal isomorphisms of the exterior can be written explicitly enough for rigorous harmonic cap computation. To the best of our knowledge, this is also the only family of Jordan arcs that are proved to be harmonically non-planar through explicit computation.

A **wedge** $W_\theta$ is a planar shape consisting of two equal-length line segments joined at one endpoint at an angle $\theta\pi$ (see Figure 1.1). A canonical model of the wedge is

$$W_\theta = \{z \in \mathbb{C} \mid z = re^{i\alpha\pi} \text{ where } r \in [0,1] \text{ and } \alpha = 0 \text{ or } \theta\}.$$

for $\theta \in (0,1]$. The result of this study is the next theorem.

**Theorem 1.4.** *A Schwarz-Christoffel exterior map* $f\colon \mathbb{D} \to \hat{\mathbb{C}} \setminus W_\theta$ *is given by*

$$f(z) = C \int_0^z \zeta^{-2} \Big( \frac{1-\zeta}{1+\zeta} \Big)^{\theta-1} (1-\omega^{-1}\zeta)(1-\omega\zeta)\, d\zeta, \tag{1.2}$$

*where* $\omega = (1-\theta) + i\sqrt{1-(1-\theta)^2}$, *and* $C = -\theta^{-\theta/2}(2-\theta)^{\theta/2-1}$. *Furthermore,* $W_\theta \cap [0,1]$ *can be parametrized by harmonic measure with respect to conformal angle* $t \in [0,\pi]$ *as*

$$F_\theta(t) = f(\gamma(t)) = 2\theta^{-\theta/2}(2-\theta)^{\theta/2-1} \sin(t/2)^\theta \cos(t/2)^{2-\theta}. \tag{1.3}$$

*The parametrization of* $W_\theta \cap e^{i\theta\pi}[0,1]$ *can be described by symmetry.*

Equation 1.3 is essentially an inverse distribution function of the harmonic measure of $W_\theta$. It allows us to show that $W_\theta$ is not harmonically planar. This is the first example shown to be harmonically non-planar through explicit computation.

**1.1.3. The cap construction algorithm.** Given a polygon $P$ and a probability measure $\mu$ supported on the vertices of $P$, the cap construction algorithm attempts to generate the cap $P'$, in the context of the questions at the beginning of the section. If $P'$ does not exist, the algorithm would generate a polygonal line that either crosses itself or does not close up to form a polygon. Based on the cap construction algorithm and numerical approximation algorithms for conformal isomorphisms [**7, 8, 13, 14**], we develope an algorithm to find the harmonic cap of a given planar shape.

## 1.2. Organization

This thesis consists of eight chapters, including this introduction. In Chapter 2, we introduce some preliminary information of the harmonic measure and present some convergence results. Chapter 3 defines harmonic caps, and provides plentiful examples of planar shapes together with their harmonic caps. Chapter 4 introduces the concept of harmonic planarity, and gives a proof of Theorems 1.1 on Jordan domains. Chapter 5 revisits harmonic planarity, focusing on Jordan arcs, and gives proofs of Theorem 1.2 and Lemma 1.3. Chapter 6 introduces the Schwarz-Christoffel transformation and its application on the computations about the wedge family, providing a rigorous computational proof of Theorem 1.4. Chapter 7 includes descriptions of the cap construction algorithm and the numerical approximation algorithms for harmonic caps, together with the zipper algorithm developed by Marshall. The last chapter presents two iterative processes related to harmonic caps, provides numerical examples of the iterative processes, and formulates a conjecture on the iterative harmonic caps.

## 1.3. Convention and Notations in this Text

- The open ball of radius $r$ centered at $x$ is denoted by $B(x, r)$. Its closure is denoted by $\overline{B}(x, r)$.
- The unit disk $\{z \in \mathbb{C} : |z| < 1\}$ is denoted by $\mathbb{D}$; the closed unit disk $\{z \in \mathbb{C} : |z| \leq 1\}$ is denoted by $\overline{\mathbb{D}}$; the upper-half plane $\{z \in \mathbb{C} : \mathrm{Im}(z) > 0\}$ is denoted by $\mathbb{H}$.
- The Riemann sphere, topologically describing the one-point compactification of the complex numbers $\mathbb{C}$, is denoted by $\hat{\mathbb{C}}$ in this text.

- For a bounded domain $\Omega$, its harmonic measure $\mu_\Omega$ will refer to the harmonic measure of the complement $\hat{\mathbb{C}}\setminus\Omega$ with respect to the point at $\infty$. When the context is clear, the subscript indicating the bounded domain will be omitted, and we simply write $\mu$. Harmonic measures with different points of reference will always be clearly indicated in this text.
- For a planar shape $P$ and a probability measure $\nu$ supported on $\partial P$, the cap of $P$ associated with $\nu$ is denoted by $\hat{P}_\nu$. Specifically, if $\nu$ is the harmonic measure $\mu_P$, the subscript indicating the measure will be omitted, and we simply write $\hat{P}$ for the harmonic cap of $P$.
- Jordan domains are usually considered open subsets of $\mathbb{C}$ or $\mathbb{R}^2$. By definition, planar shapes are compact, therefore closed in the plane. In this text, when a Jordan domain $\Omega$ is designated as a planar shape, we always take the closure $\overline{\Omega}$ of the Jordan domain as the planar shape to work with.
- A Jordan arc is the image of an injective continuous function $\gamma\colon [0,1]\to\mathbb{C}$. In this text, Jordan arcs are never self-intersecting. The endpoints of a Jordan arc are always distinct.
- The *Riemann Mapping Theorem* asserts the existence of a conformal isomorphism from the unit disk to any simply connected proper subset of $\mathbb{C}$. In this text, we use the words "Riemann map" and "conformal isomorphism" interchangeably to refer to a biholomorphic function from either $\mathbb{D}$ or $\hat{\mathbb{C}}\setminus\overline{\mathbb{D}}$ to a simply connected proper subset of $\mathbb{C}$, or the inverse of such a function.

CHAPTER 2

# The Harmonic Measure

This chapter includes the preliminaries required for the thesis. It mainly consists of fundamental knowledge about harmonic measures and its connection to a few different branches of mathematics.

## 2.1. Definitions of the Harmonic Measure

Let $P$ be a planar shape. The **harmonic measure** $\mu_P$ of $P$ (with respect to the point at $\infty$) is given by the pushforward $\mu_P = \Phi_*\lambda$, where $\lambda$ is the normalized arclength measure on $\partial\mathbb{D}$, and $\Phi\colon\ \hat{\mathbb{C}}\setminus\overline{\mathbb{D}} \to \hat{\mathbb{C}}\setminus P$ is a conformal isomorphism that fixes the point at $\infty$ [**11**]. There are quite a few equivalent definitions of the harmonic measure for planar shapes.

An intuitive definition of harmonic measure is given in terms of boundary hitting distribution of Brownian motions. Let $B_t$ be a standard Brownian motion starting at $z \in \mathbb{C}\setminus P$, and let $T$ be the first hitting time of the Brownian motion into $\partial P$. Let $E \subseteq \partial P$ be a measurable set. For a point $z \in \mathbb{C}\setminus P$, the function

$$\mathbb{P}_z(B_T \in E \mid T < \infty)$$

is a harmonic function in $z$, and the harmonic measure is given by

$$\mu_B(E) = \lim_{z\to\infty} \mathbb{P}_z(B_T \in E \mid T < \infty),$$

for all measurable $E \subseteq \partial P$.

From the potential-theoretic point of view, the harmonic measure is the energy-minimizing measure on $P$, sometimes also referred to as the **equilibrium measure**. Let $\mathcal{P}(P)$ be the collection of Borel probability measures on $P$, and let the **energy** of $\nu \in \mathcal{P}(P)$ be defined by

$$I(\nu) = -\iint \log|z-w|\, d\nu(w)\, d\nu(z).$$

Then the harmonic measure $\mu_E$ is the unique measure that satisfies

$$I(\mu_E) = \inf_{\nu \in \mathcal{P}(P)} I(\nu).$$

Next we consider the Dirichlet problem on $P$. Every $f \in C(\partial P)$ has an extension $h_f \in C(\overline{\hat{\mathbb{C}} \setminus P})$ that is harmonic in $\hat{\mathbb{C}} \setminus P$. The map $f \to h_f(\infty)$ is therefore a positive linear functional on $C(\partial P)$. By the Riesz representation theorem,

$$h_f(\infty) = \int_{\partial P} f\, d\mu_R$$

for some Radon measure $\mu_R$ on $\partial P$, and this measure $\mu_R$ is the harmonic measure of $P$.

**Theorem 2.1.** *The measures $\mu_P$, $\mu_B$, $\mu_E$, and $\mu_R$ defined above are all equivalent.*

Equivalence of these definitions of harmonic measure are classical results. Proofs can be found in various texts [**11, 15, 17**]. As mentioned in section 1.3, we simply write $\mu$ for the harmonic measure in this text when the context is clear.

## 2.2. Convergence of Harmonic Measures

In 2019, Binder *et al.* showed in [**3**] that weak convergence of harmonic measure with respect to an interior point is equivalent to *Caratheódory convergence* of the underlying domains.

**Definition 2.2** (Carathéodory Convergence)**.** Let $(\Omega_n, x_n)$ and $(\Omega, x)$ be pointed simply connected domains in $\mathbb{C}$. We say that $(\Omega_n, x_n) \to (\Omega, x)$ **converges in the Carathéodory sense** if

(1) $x_n \to x$;

(2) for any compact $K \subseteq \Omega$, we have $K \subseteq \Omega_n$ for all $n$ sufficiently large;

(3) for any open connected $U$ containing $x$, if $U \subseteq \Omega_n$ for infinitely many $n$, then $U \subseteq \Omega$.

**Example 2.3.** Let $\{a_n\}$ be a real-valued sequence that converges to 1. Then $(\mathbb{D}_{a_n}, 0) \to (\mathbb{D}, 0)$ in the Carathéodory sense.

**Remark 2.4.** The example above presents a sequence of domains converging not only in the Carathéodory sense, but also in the Hausdorff metric. Convergence in the Carathéodory sense is strictly weaker than Hausdorff convergence, as demonstrated in the next example.

**Example 2.5.** Let $\Omega = \mathbb{D}$, and let

$$\Omega_n = \mathbb{D} \cup \{z \in \mathbb{C} \mid 0 < \operatorname{Re}(z) < 2, \text{ and } |\operatorname{Im}(z)| < 1/n\}.$$

Then $(\Omega_n, 0) \to (\Omega, 0)$ in the Carathéodory sense. In this example, the sequence does not converge in the Hausdorff metric. The Hausdorff distance $d_H(\Omega_n, \Omega) \geq 1$ for every natural number $n$ because of the spike along the direction of the positive real axis.

**Definition 2.6** (Arbitrarily Good Common Interior Approximations)**.** Let $x \in \mathbb{C}$, and let $\Omega_n$ and $\Omega$ be simply connected bounded domains containing $x$. We say that $\Omega_n$ and $\Omega$ have **arbitrarily good common interior approximations** if for all $\epsilon > 0$, there exists $N \in \mathbb{N}$ and $K_\epsilon \subseteq \Omega \cap \bigcap_{n \geq N} \Omega_n$ containing $x$ such that

$$d(y, \partial\Omega) < \epsilon \quad \text{and} \quad d(y, \partial\Omega_n) < \epsilon$$

for all $y \in \partial K_\epsilon$.

The following theorem proved by Binder *et al.* shows the equivalence among weak convergence of harmonic measures, arbitrarily good common interior approximation, and Carathéodory convergence.

**Theorem 2.7.** *Let $(\Omega_n, x_n)$ and $(\Omega, x)$ be pointed simply connected domains in $\mathbb{C}$. Let $\omega_n$ denote the harmonic measures of $\Omega_n$ with respect to $x_n$, and $\omega$ denote the harmonic measure of $\Omega$ with respect to $x$. The followings are equivalent:*

(1) *The sequence of harmonic measures $\omega_n$ converges to $\omega$ in the weak sense.*

(2) *$(\Omega_n, x_n) \to (\Omega, x)$ in the Carathéodory sense.*

(3) *$(\Omega_n, x_n)$ and $(\Omega, x)$ have arbitrarily good common interior approximation.*

One classical result of Carathéodory [**10**] states that

**Theorem 2.8** (Carathéodory Kernel Theorem)**.** *Let $(\Omega_n, x_n)$ and $(\Omega, x)$ be pointed simply connected domains in $\mathbb{C}$. Let $\Phi_n \colon \mathbb{D} \to \Omega_n$ be conformal maps with $\Phi_n(0) = x_n$ and $\Phi_n'(0) > 0$, and let $\Phi \colon \mathbb{D} \to \Omega$ be the conformal map with $\Phi(0) = x$ and $\Phi'(0) > 0$. Then $\Phi_n \to \Phi$ on compact subsets of $\mathbb{D}$ if and only if $(\Omega_n, x_n) \to (\Omega, x)$ in the Carathéodory sense.*

A special case of Theorem 2.7 and 2.8 gives us the following corollary characterizing weak convergence of harmonic measures (with respect to the point at $\infty$).

**Corollary 2.9.** *Let $P_n$ and $P$ be planar shapes, and let $\mu_n$ and $\mu$ be their respective harmonic measures. Let $\Phi_n \colon \hat{\mathbb{C}} \setminus \overline{\mathbb{D}} \to \hat{\mathbb{C}} \setminus P_n$ and $\Phi \colon \hat{\mathbb{C}} \setminus \overline{\mathbb{D}} \to \hat{\mathbb{C}} \setminus P_n$ be conformal isomorphisms with $\Phi_n(\infty) = \infty$ and $\Phi_n'(\infty) > 0$. Then the followings are equivalent:*

(1) *$\Phi_n \to \Phi$ on compact subsets of $\mathbb{D}$.*

(2) *$\mu_n \to \mu$ in the weak sense.*

(3) *$(\hat{\mathbb{C}} \setminus P_n, \infty) \to (\hat{\mathbb{C}} \setminus P, \infty)$ in the Carathéodory sense.*

This result allows us to use the harmonic measure of domains converging in the Carathéodory sense as an approximation of harmonic measure. In practice, we can use the harmonic measure of domains that are Hausdorff-close to the target domain as an approximation, because Hausdorff convergence is stronger than Carathéodory convergence.

## 2.3. Convergence of Conformal Metrics

One classical result by Reshetnyak [**18**] in 1960 is a theorem on the convergence of metrics. In a neighborhood of each point of a two-dimensional Riemannian manifold, we can introduce an *isothermal* coordinate system in which the metric quadratic form of the

manifold is

$$ds^2 = \lambda(x,y)(dx^2 + dy^2) = \lambda(z)\,|dz|^2.$$

The function $\lambda(z)$ is expressed in terms of the integral curvature of the Riemannian manifold by the formula

$$\lambda(z) = \exp\Big[\frac{1}{\pi}\int_G \ln\frac{1}{|z-\zeta|}\,d\omega(\zeta) + h(z)\Big], \tag{2.1}$$

where $G \subseteq \mathbb{C}$ is the range of values for the given coordinate system, and $h(z)$ is a harmonic function. Let $G \subseteq \mathbb{C}$ be a bounded domain. Assume that there is a measure $\omega$ and a harmonic function $h$ specified in $G$. We put

$$\lambda(z;\omega,h) = \exp\Big[\frac{1}{\pi}\int_G \ln\frac{1}{|z-\zeta|}\,d\omega(\zeta) + h(z)\Big].$$

The function $\lambda(z;\omega,h)$ is finite for almost every $z \in G$. It is closely connected with the class of *subharmonic* functions. In fact, $-\ln\lambda(z)$ is subharmonic if $\omega$ is a non-negative measure. Now let $z_1, z_2 \in G$, and define

$$\rho_\lambda(z_1,z_2) = \inf_K \int_K \sqrt{\lambda(z)}\,|dz|, \tag{2.2}$$

where the infimum is taken on the set of all rectifiable curves $K$ contained in $G$ joining the points $z_1$ and $z_2$. It is possible that $\rho_\lambda(z_0,z) = \infty$ for some points $z_0 \in G$, no matter where $z \in G\backslash\{z_0\}$ is. If $z_0$ has this property, it is called a *point at infinity* with respect to the conformal metric line element $\lambda(z)\,|dz|^2$. The following theorem by Reshetnyak shows that the function $\rho_\lambda$ defined above is a metric intrinsic to $G$.

**Theorem 2.10.** *Suppose that a function $\lambda(z) = \lambda(z; \omega, h)$ is specified in a domain $G \subseteq \mathbb{C}$. Let $\tilde{G}$ be the domain obtained from $G$ by excluding the points at infinity with respect to the line element $\lambda(z)\,|dz|^2$. Then the function $\rho_\lambda(z_1, z_2)$ is the intrinsic metric in $\tilde{G}$ compatible with the topology of $\tilde{G}$ as a subset of $\mathbb{C}$, and the metric space $(\tilde{G}, \rho_\lambda)$ is a two-dimensional manifold of bounded curvature.*

The converse of this theorem also holds true.

**Theorem 2.11.** *Let $M$ be a two-dimensional manifold of bounded curvature. Any point $p \in M$ has a neighborhood $U$ which is isometric to some flat domain $G$ with a metric $\rho$ in $G$ that can be defined from some function $\lambda(z)$ of the form (2.1).*

The next theorem is Reshetnyak's result that weak convergence of curvature distributions as measures implies convergence of conformal metrics.

**Theorem 2.12.** *Let $\omega_n$ be non-negative measures defined in the domain $G$ and weakly converging to the measure $\omega$ in $G$. Let $\lambda_n(z) = \lambda(z; \omega_n)$, and $\lambda(z) = \lambda(z; \omega)$. Then the functions $\rho_{\lambda_n}(z, \zeta)$ converge to the function $\rho_\lambda(z, \zeta)$ uniformly on any closed subset of $G$ not containing points at infinity with respect to $\lambda(z)\,|dz|^2$.*

Applying this theorem to the setting of harmonic caps, it allows us to use approximated harmonic measures as curvature distributions, while still providing good approximations on the metric of $(\hat{\mathbb{C}}, \rho)$, provided that the metrized sphere exists for the setting of the harmonic cap question at the beginning of Chapter 1.

CHAPTER 3

# Harmonic Caps and Examples

Recall the question proposed in Chapter 1: given a probability measure $\mu$ supported on $\partial P$, does there exist a conformal metric $\rho = \rho(z)|dz|$ on the Riemann sphere $\hat{\mathbb{C}}$ such that

(1) $P$, with Euclidean metric, embeds locally-isometrically into $(\hat{\mathbb{C}}, \rho)$; and
(2) The curvature distribution on $(\hat{\mathbb{C}}, \rho)$ equals the pushforward of $4\pi\mu$ under the said embedding?

In 2017, DeMarco and Lindsey [**6**] proved the existence of such a conformal metric $\rho$ for any planar shape $P$ with its harmonic measure $\mu$ as the given probability measure. The complement of $P$ in the metrized sphere $(\hat{\mathbb{C}}, \rho)$ is the **harmonic cap** of $P$, denoted by $\hat{P}$. Further, they presented the locally univalent function $g\colon \mathbb{D} \to \mathbb{C}$ defined by

$$g(z) = \int_0^z \Phi'(1/x)\, dx, \tag{3.1}$$

where $\Phi\colon \hat{\mathbb{C}} \setminus \overline{\mathbb{D}} \to \hat{\mathbb{C}} \setminus P$ is a conformal isomorphism fixing $\infty$, as a parametrization of the Euclidean development of the harmonic cap $\hat{P}$. It is worth mentioning that $g$ is only guaranteed to be locally one-to-one, which means that the development of $\hat{P}$ may not be able to embed into $\mathbb{C}$. In this thesis, we will exclusively consider globally one-to-one development of harmonic caps (c.f. [**6**, §2.3]). All the planar shapes that appear in this thesis have planar harmonic caps. If we further assume that $P$ has rectifiable boundary,

a *perimeter gluing* of $P$ and $\hat{P}$ can be performed with boundary identification by arc length. Given $s(t) = \int_0^t e^{i\alpha(x)}\,dx$ a counterclockwise arc-length parameterization of $\partial P$, the boundary of $\hat{P}$ is parameterized clockwise by

$$\hat{s}(t) = \int_0^t e^{i(\alpha(x)-\kappa(x))}\,dx, \tag{3.2}$$

where $\kappa(t) = 4\pi\mu(s[0,t])$, and the perimeter gluing is given by the boundary identification $s(t) \sim \hat{s}(t)$.

The metrized sphere $(\hat{\mathbb{C}}, \rho)$ has non-negative curvature proportional to the distribution of the harmonic measure of $P$. Alexandrov's uniqueness theorem [**1**] asserts that $(\hat{\mathbb{C}}, \rho)$ is isometric to the boundary surface of a bounded convex subset of $\mathbb{R}^3$. Because the harmonic measure is only supported on the boundary of $P$, the interior of $\hat{P}$ is flat, and can be isometrically embedded in $\mathbb{R}^2$ or $\mathbb{C}$. Equation 3.1 provides such an embedding. On the other hand, Equation 3.2 lays the foundation of the cap construction algorithm, which will be introduced in detail in Chapter 7. Despite these positive results in generating developments of harmonic caps, it is difficult to determine the structure of the convex realization from a development. Algorithms only exist in certain polyhedral metric cases, *i.e.*, spheres with discrete curvature [**4**].

A direct computation shows that the metric $\rho$ is invariant under rotation, scaling, and translation of the planar shape.

**Lemma 3.1.** *Let $P$ and $Q$ be planar shapes, and suppose that $Q$ can be obtained from $P$ with only rotation, scaling, and translation in the plane, then the corresponding harmonic caps $\hat{P}$ and $\hat{Q}$ are the same up to rotation, scaling, or translation.*

PROOF. Let $\Phi_P\colon \hat{\mathbb{C}}\setminus\overline{\mathbb{D}} \to \hat{\mathbb{C}}\setminus P$ is a conformal isomorphism fixing $\infty$. If $Q$ can be obtained from $P$ with only rotation, scaling, and translation in the plane, then a conformal isomorphism $\Phi_Q\colon \hat{\mathbb{C}}\setminus\overline{\mathbb{D}} \to \hat{\mathbb{C}}\setminus Q$ can be constructed by

$$\Phi_Q(z) = \alpha \cdot \Phi_P(z) + \beta$$

for some appropriate choices of $\alpha \in \mathbb{C}\setminus\{0\}$ and $\beta \in \mathbb{C}$. Furthermore, this construction of $\Phi_Q$ fixes the point at $\infty$. Thus $\hat{Q}$ can be parameterized by

$$g_Q(z) = \int_0^z \Phi_Q'(1/x)\,dx = \int_0^z \alpha \cdot \Phi_P'(1/x)\,dx = \alpha \cdot g_P(z).$$

Hence, $\hat{P}$ and $\hat{Q}$ differ by at most a rotation and a scaling. □

The short argument above tells us that every example of harmonic cap is in fact a representative of a family of harmonic caps, in the sense that SO(2) actions on the planar shape does not affect the conformal metric $\rho$ on the Riemann sphere $\hat{\mathbb{C}}$.

We now present several examples of planar shapes and their corresponding harmonic caps. We also attempt to reconstruct some of the convex realizations from the Euclidean developments, using paper cut-outs and tape.

**Example 3.2.** The simplest example is $P = \overline{\mathbb{D}}$ the closed unit disk. The harmonic measure is precisely the normalized arclength measure on $\partial\mathbb{D}$, with corresponding conformal isomorphism $\Phi(z) = z$. Using Equation 3.1, the harmonic cap of $\overline{\mathbb{D}}$ can be parametrized by

$$g(z) = \int_0^z \Phi'(1/x)dx = \int_0^z dx = z,$$

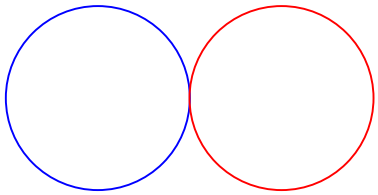

Figure 3.1. The unit disk and its harmonic cap

which means that the harmonic cap of the unit disk is the disk itself. Figure 3.1 shows the unit disk (blue) together with its harmonic cap (red). In this thesis, all figures showing a planar shape together with its harmonic cap have the original planar shape in blue and its harmonic cap in red, unless otherwise indicated. Perimeter gluing of the disk and its harmonic cap identifies points on these two unit circles by arc length, which results in a double cover of the disk as the convex realization.

**Example 3.3.** Let $P$ be a line segment. First of all, a line segment is a planar shape, as it is (1) compact, (2) connected, and (3) contains at least two points. Without loss of generality, assume $P = [-2, 2] \subseteq \mathbb{R} \subseteq \mathbb{C}$. Then a conformal isomorphism $\Phi\colon \hat{\mathbb{C}} \setminus \overline{\mathbb{D}} \to \hat{\mathbb{C}} \setminus P$ fixing the point at $\infty$ could be

$$\Phi(z) = z + \frac{1}{z}$$

Thus the harmonic cap of $P$ can be parametrized by the function $g\colon \mathbb{D} \to \mathbb{C}$ with

$$g(z) = \int_0^z \Phi'(1/x)\, dx = \int_0^z 1 - x^2\, dx = z - \frac{z^3}{3}.$$

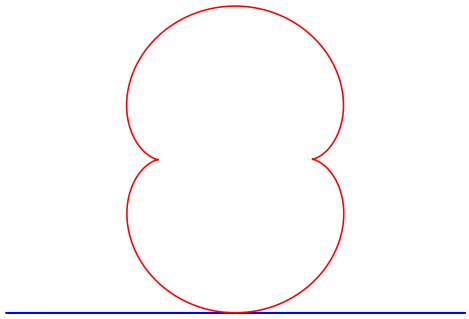

Figure 3.2. A line segment and its harmonic cap

Its harmonic cap is shown in Figure 3.2. Perimeter gluing uses the line segment itself as the glue, and paste the reflectively symmetric parts of the harmonic cap together to form a double cover of half of the harmonic cap as the convex realization.

**Example 3.4.** The conformal isomorphism in Example 3.3 is the Joukowsky transform, which maps circles centered at the origin to ellipses with foci $\pm 2$. Thus, it can be used to construct conformal isomorphisms for ellipses of all eccentricity. Let $a > 1$, and

$$\Phi_a(z) = az + \frac{1}{az}$$

Then $\Phi_a \colon \hat{\mathbb{C}} \setminus \overline{\mathbb{D}} \to \hat{\mathbb{C}} \setminus E_a$ is a conformal isomorphism for an ellipse $E_a$. The harmonic cap of $E_a$ can be parametrized by the function $g_a \colon \mathbb{D} \to \mathbb{C}$ with

$$g_a(z) = \int_0^z \Phi_a'(1/x)\, dx = \int_0^z a - \frac{x^2}{a}\, dx = az - \frac{z^3}{3a}.$$

Some ellipses and their corresponding harmonic caps are shown in Figure 3.3. With ellipses, the convex realizations are no longer of zero volume. Paper cut-outs of ellipses and their harmonic caps can be glued along their boundary and provide an insight into

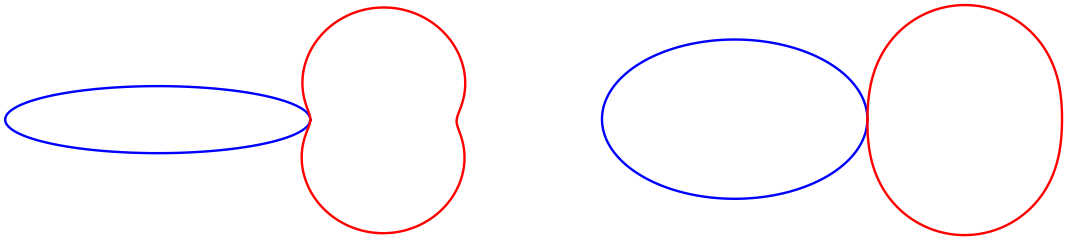

Figure 3.3. Ellipses and their corresponding harmonic caps

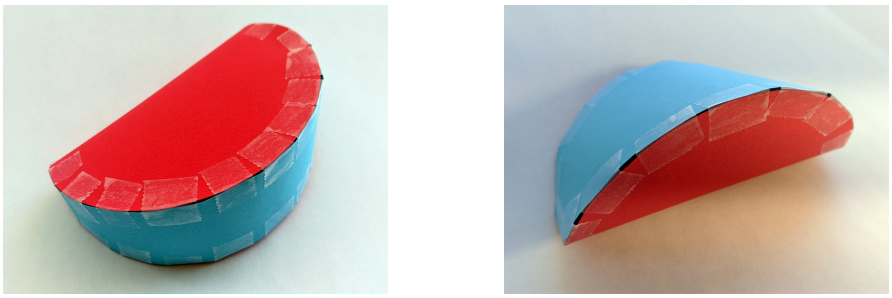

Figure 3.4. The paper cut-outs of ellipses and their harmonic caps paste together along their boundaries to form corresponding convex realizations.

the shape of the actual convex realizations. Images of these paper cut-outs are included in Figure 3.4.

**Example 3.5.** The harmonic cap of $P = [0, 1] \cup [0, 1]i$ can be computed explicitly with Schwarz-Christoffel transformations. It is shown in Figure 3.5. Details can be found in Chapter 6.

All examples above are computed explicitly either with Equation 3.1 or by boundary parametrization. The next few examples are numerical. The harmonic measures are obtained by the zipper algorithm, and the harmonic caps are constructed with the cap construction algorithm. All curved sides in the figures are in fact polygonal lines. Descriptions of both algorithms can be found in Chapter 7.

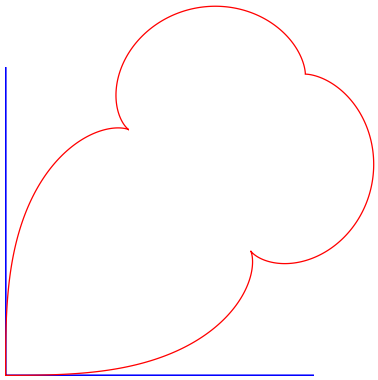

Figure 3.5. The right-angle wedge and its harmonic cap

**Example 3.6.** The harmonic caps of a square, a rhombus, a semicircular disk, and a hexagon are shown in Figure 3.6.

**Example 3.7.** The harmonic caps of semicircular arches with different thickness were also computed. They are shown in Figure 3.7. The paper cut-outs of these planar shapes and their harmonic caps glue together to form almost flat empanada-like convex bodies,

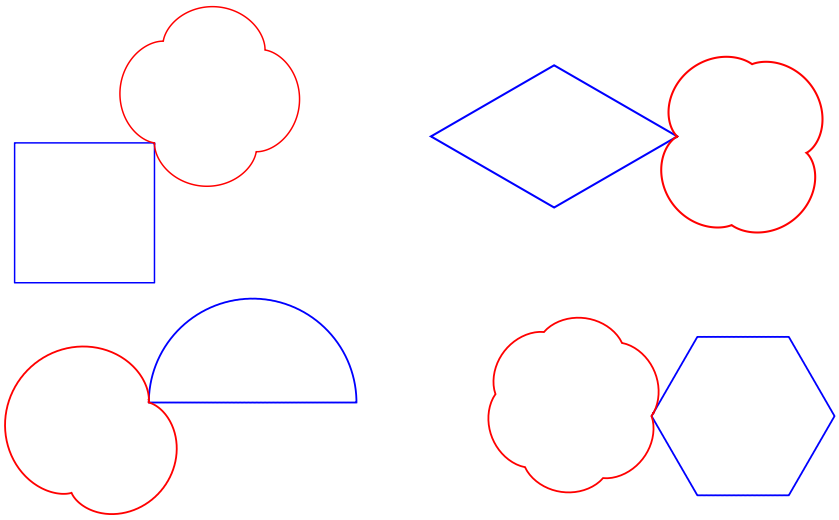

Figure 3.6. Different shapes and their corresponding harmonic caps

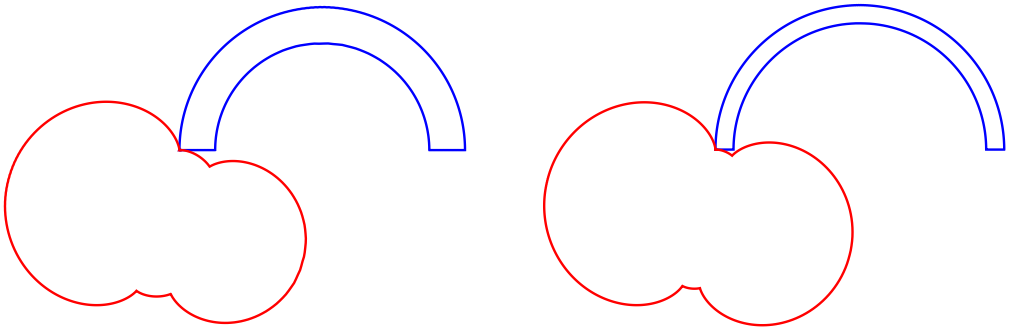

Figure 3.7. Semicircular arches and their corresponding harmonic caps

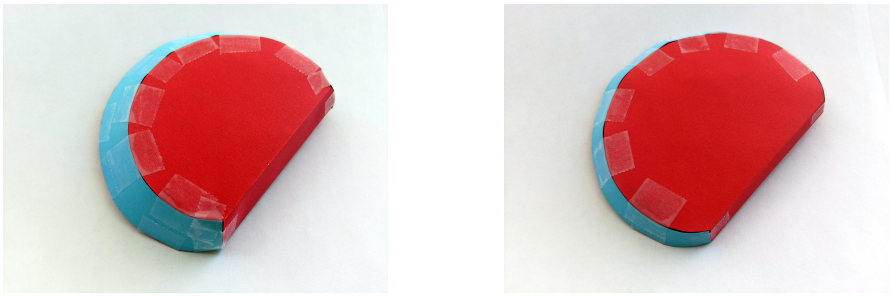

Figure 3.8. The paper cut-outs of the semicircular arches and their harmonic caps form almost flat convex bodies.

whose images are included in Figure 3.8. It was these harmonic cap figures that led to suspicion and eventual proof that circular arcs are harmonically planar.

**Example 3.8.** The cap construction algorithm is capable of computing the harmonic caps of fairly complicated planar shapes. Figure 3.9 shows an approximation of the cauliflower Julia set (the filled Julia set of $f(z) = z^2 + 1/4$) together with its harmonic cap development. The planar shape is a polygonal approximation by 2048 vertices on the Julia set.

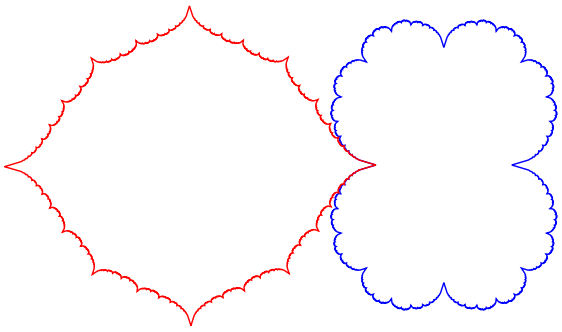

Figure 3.9. The cauliflower Julia set (blue) and its harmonic cap (red)

Convergence of harmonic caps is worth mentioning at the end of this chapter. Carathéodory kernel theorem (2.8) states that locally uniform convergence of Riemann maps is equivalent to Carathéodory convergence of planar shapes. Since the development of harmonic caps can be parameterized by an integral of the Riemann map, as stated in Equation 3.1, we expect harmonic caps to converge on compact subsets as we take a sequence of planar shapes converging in the Carathéodory sense.

**Lemma 3.9.** *Let $P_n$ be a sequence of planar shapes that converge in the Carathéodory sense to a planar shape $P$. Then the harmonic caps $\hat{P}_n$ also converge in the Carathéodory sense, and the limit is $\hat{P}$.*

CHAPTER 4

# Harmonic Planarity of Jordan Domains

The results in [**6**] showed the existence of a metrized sphere $(\hat{\mathbb{C}}, \rho)$ realizing the gluing of any planar shape $P$ with its harmonic cap $\hat{P}$ along the boundary. Examples 3.2 and 3.3 have already demonstrated that some special planar shapes have a doubly-covered convex planar region as the realization of such gluing. In this chapter, we investigate the criterion for a Jordan domain to be *harmonically planar*.

## 4.1. First Take on Jordan Domains

We have seen in Example 3.2 that the harmonic cap of the unit disk is the disk itself, and the convex realization formed by gluing $\overline{\mathbb{D}}$ and its harmonic cap is a doubly covered disk.

This is an interesting scenario, as the convex body resulted from perimeter gluing of the planar shape and its harmonic cap is entirely contained in a plane. We say such planar shapes, whose corresponding metrized sphere $(\hat{\mathbb{C}}, \rho)$ is entirely contained in a plane, are **harmonically planar**.

The first step is to identify all harmonically planar Jordan domains that are smoothly bounded. The bonus for assuming smooth boundary is that the conformal isomorphism $\Phi\colon \hat{\mathbb{C}} \setminus \overline{\mathbb{D}} \to \hat{\mathbb{C}} \setminus P$ can be smoothly extended to the boundary, which enables us to use derivatives in the argument. The following proposition characterizes all of them using Equation 3.2.

**Proposition 4.1.** *Let $P \subseteq \mathbb{C}$ be a Jordan domain with smooth boundary. Then $P$ is harmonically planar if and only if $P$ is a disk.*

PROOF. Let $s\colon [0, L] \to \mathbb{C}$ be a counter-clockwise unit-speed parameterization of $\partial P$. Without loss of generality, assume that $s(0) = 0$ and $s'(0) = i$. Write $s(t) = \int_0^t e^{i\alpha(x)}\, dx$ for a smooth function $\alpha\colon [0, L] \to \mathbb{R}$. Then $s'(t) = e^{i\alpha(t)}$. Assume that $\alpha(0) = \pi/2$. Let $\Phi\colon \hat{\mathbb{C}} \setminus \overline{\mathbb{D}} \to \hat{\mathbb{C}} \setminus P$ be a conformal isomorphism with $\Phi(\infty) = \infty$. Regularity of $\partial P$ guarantees that $\Phi$ extends smoothly to $\partial\, \mathbb{D}$. Define $\theta(t) = \arg(\Phi^{-1}(s(t)))$. Assume that $\Phi$ satisfies $\theta(0) = 0$, or equivalently, $\Phi(1) = 0$. Then

$$\hat{s}(t) = \int_0^t e^{i(\alpha(x) - 2\theta(x))}\, dx,$$

and $\hat{s}'(t) = e^{i(\alpha(t) - 2\theta(t))}$. Assume that $P$ and $\hat{P}$ differs by a reflection across the imaginary axis, so that $P$ could be harmonically planar, then

$$\hat{s}'(t) = -\overline{s'(t)},$$

or equivalently,

$$e^{i(\alpha(t) - 2\theta(t))} = -e^{-i\alpha(t)} = e^{i(-\alpha(t) + \pi)}.$$

Thus $\theta(t) = \alpha(t) - \pi/2$. By construction, we have

$$\Phi(e^{i\theta(t)}) = s(t) = \int_0^t e^{i\alpha(x)}\, dx = \int_0^t e^{i(\theta(x) + \pi/2)}\, dx = i \int_0^t e^{i\theta(x)}\, dx.$$

Take $t$-derivatives on both sides, we get

$$\Phi'(e^{i\theta(t)}) \cdot i\theta'(t) e^{i\theta(t)} = i e^{i\theta(t)}.$$

Hence, $\Phi'(e^{i\theta(t)})\cdot\theta'(t) = 1$. But $\theta(t)$ is a real-valued function, so is $\theta'(t)$, which implies that $\Phi'(z) \in \mathbb{R}$ for all $|z| = 1$. Because $\Phi'(z)$ is holomorphic on $\hat{\mathbb{C}}\setminus\overline{\mathbb{D}}$, we have $\mathrm{Im}(\Phi')$ harmonic on $\hat{\mathbb{C}}\setminus\overline{\mathbb{D}}$, and $\mathrm{Im}(\Phi') = 0$ on $\partial\,\mathbb{D}$. By maximum principle, $\mathrm{Im}(\Phi') = 0$ throughout $\hat{\mathbb{C}}\setminus\overline{\mathbb{D}}$. Cauchy-Riemann equation indicates that $\Phi'(z)$ is a real constant. It follows that $P$ is an affine transformation of $\mathbb{D}$.

The converse has been demonstrated in Example 3.2. □

## 4.2. General Jordan Domains

Any Jordan domain can be approximated by smoothly-bounded Jordan domains, where the approximation is achieved in the sense of Hausdorff. Convergence of harmonic measures guarantees that the harmonic caps of the approximating domains also approximates the actual harmonic cap. This alludes to a stronger version of Proposition 4.1 for general Jordan domains, which is the statement of Theorem 1.1.

**Theorem 1.1.** *Let $P \subseteq \mathbb{C}$ be the closure of a Jordan domain. Then $P$ is harmonically planar if and only if $P$ is a closed circular disk.*

The "if" part of the theorem is clear from the computation in Example 3.2. To prove the "only if" part, we first observe that the unique convex realization of the metrized sphere $(\hat{\mathbb{C}}, \rho)$ with respect to $P$ and its harmonic measure $\mu$ is obtained by identifying $P$ and $\hat{P}$ along the boundary, which results in both $P$ and $\hat{P}$ isometrically embedded into the same plane, forming a two-sheeted double of $P$ that is a degenerate topological sphere contained within a plane. The Alexandrov realization of the metrized sphere $(\hat{\mathbb{C}}, \rho)$ is convex in $\mathbb{R}^3$, and is also contained in a plane. It follows that $P$ itself is a convex Jordan domain. We first state a few preliminary lemmas.

**Lemma 4.2.** *Convex Jordan domains have rectifiable boundary.*

This result is classical. A proof can be found in [**21**, §1.5]. Here we present a proof that uses a similar argument, but with a more explicit computation.

PROOF. Let $P$ be a convex Jordan domain. Let $p_0, p_1, \ldots, p_{n-1}, p_n = p_0$ be an arbitrary sequence of points in order on $\partial P$. By convexity of $P$, each line segment $[p_{k-1}, p_k]$ is contained in $P$. Further, the inner incident angle at the point $p_k$ is not greater than $\pi$. Thus the polygonal line joining $p_0$ through $p_n$ forms the boundary of a convex polygon $\Pi$. Let $R$ be a rectangle that satisfies (1) its sides are parallel to the coordinate axes, and (2) it encloses $P$. Then $R$ encloses the polygon $\Pi$. Project each segment $S_k = [p_{k-1}, p_k]$ horizontally and vertically onto $R$ so that the projections are in the direction away from $\Pi$. Let segments $H_k$ and $V_k$ be the respective results of the projections. Because $\Pi$ is convex, every horizontal line has at most two points of intersection with $\Pi$, so does every vertical line. Therefore, the segments $\{H_k\}$ and $\{V_k\}$ are pairwise disjoint (except possibly at

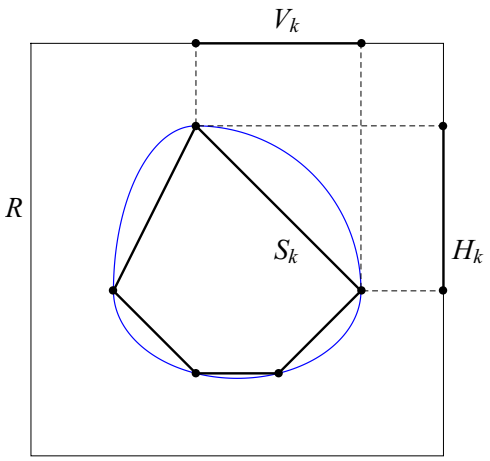


Figure 4.1. The circumference of a convex Jordan domain is bounded by a rectangle.

endpoints), and $\ell(S_k) \leq \ell(H_k) + \ell(V_k)$. Therefore,

$$\ell(\Pi) \leq \sum_{k=1}^{n} \ell(H_k) + \ell(V_k) \leq \ell(R).$$

Because our choice of polygonal line was arbitrary, and $R$ does not depend on this choice, we have

$$\ell(\partial P) = \sup_{\Pi} \ell(\Pi) \leq \ell(R).$$

Hence, $\partial P$ is rectifiable. □

**Lemma 4.3.** *The image of the function* $F\colon \hat{\mathbb{C}} \setminus P \to \mathbb{C}$ *defined by*

$$F(z) = \int_{\infty}^{z} \frac{1}{[\Phi^{-1}(\zeta)]^2}\, d\zeta$$

*is a Euclidean development of the harmonic cap of* $P$ *parametrized by* $z \in \hat{\mathbb{C}} \setminus P$. *Further, suppose that* $P$ *is a convex Jordan domain, and let* $\gamma(t)$ *be an arc-length parametrization of* $\partial P$. *Then* $F(\gamma(t))$ *is an arc-length parametrization of* $\partial \hat{P}$.

The proof of the first part of this lemma is in [**6**]. The argument is relatively short, and we include it in the proof later in this section for completeness. A direct consequence of this argument is the existence of harmonic caps in general.

To prove the second part, we begin with the following lemma.

**Lemma 4.4.** *Let* $D \subseteq \mathbb{C}$ *be a convex Jordan domain. Let* $f\colon \hat{\mathbb{C}} \setminus \overline{D} \to \mathbb{C}$ *be a holomorphic function with a continuous extension to* $\partial D$. *Let* $p, q \in \partial D$, *and* $\Gamma \subseteq \hat{\mathbb{C}} \setminus D$ *a*

*rectifiable curve joining $p$ to $q$. The path integral*

$$\int_\Gamma f(z)\,dz$$

*from $p$ to $q$ is independent of the choice of $\Gamma$. In particular, we may choose $\Gamma$ to be the curve $\Gamma_0$ joining $p$ to $q$ along $\partial D$.*

PROOF. It suffices to prove the case where $\Gamma$ intersects $\partial D$ only at the endpoints $p$ and $q$. Let $\gamma\colon [0, L] \to \hat{\mathbb{C}} \setminus D$ be an arc-length parametrization of $\Gamma$ with $\gamma(0) = q$ and $\gamma(L) = q$. Let $p_n = \gamma(1/n)$ and $q_n = \gamma(L - 1/n)$. Then $p_n, q_n \in \hat{\mathbb{C}} \setminus \overline{D}$, and $|p_n - p| \le 1/n$ and $|q_n - q| \le 1/n$. Because $f$ is continuous on a compact set, it is bounded. Let $B \in \mathbb{R}$ be an upper bound of $|f|$. Then

$$\left| \int_\Gamma f(z)\,dz - \int_{p_n}^{q_n} f(z)\,dz \right| \le \int_p^{p_n} |f(z)|\,dz + \int_{q_n}^{q} |f(z)|\,dz \le \frac{2B}{n} \to 0$$

as $n \to \infty$. Now let $p_n', q_n' \in \hat{\mathbb{C}} \setminus \overline{D}$ be points obtained in the same way from another curve $\Gamma'$. Then $p_n, p_n' \in B(p, 1/n)$ and $q_n, q_n' \in B(q, 1/n)$. Because $D$ is convex, we can find a path in $B(p, 1/n) \setminus \overline{D}$ joining $p_n$ to $p_n'$ with arc length at most

$$2 \cdot \frac{1}{n} + \frac{2\pi}{n} = \frac{2 + 2\pi}{n}$$

Such a path may be constructed as illustrated in Figure 4.2. Then

$$\left| \int_{p_n}^{p_n'} f(z)\,dz \right| \le \int_{p_n}^{p_n'} |f(z)|\,dz \le \frac{(2 + 2\pi)B}{n}.$$

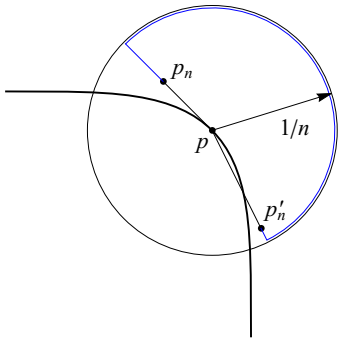


Figure 4.2. Path integral close to the endpoint on the boundary

It then follows that

$$\begin{aligned}
&\left|\int_\Gamma f(z)\,dz - \int_{\Gamma'} f(z)\,dz\right| \\
&\leq \left|\int_\Gamma f(z)\,dz - \int_{p_n}^{q_n} f(z)\,dz\right| + \left|\int_{\Gamma'} f(z)\,dz - \int_{p'_n}^{q'_n} f(z)\,dz\right| + \left|\int_{p_n}^{q_n} f(z)\,dz - \int_{p'_n}^{q'_n} f(z)\,dz\right| \\
&\leq \frac{2B}{n} + \frac{2B}{n} + \left|\int_{p_n}^{p'_n} f(z)\,dz\right| + \left|\int_{q_n}^{q'_n} f(z)\,dz\right| \\
&\leq \frac{2B}{n} + \frac{2B}{n} + \frac{(2+2\pi)B}{n} + \frac{(2+2\pi)B}{n} \\
&= \frac{(8+4\pi)B}{n} \to 0
\end{aligned}$$

as $n \to \infty$. Thus the line integral is independent of curves interior of $\hat{\mathbb{C}} \setminus D$.

Let $x \in D$, and define

$$M = \sup_{y \in \partial D} |x - y| \quad \text{and} \quad m = \inf_{y \in \partial D} |x - y|$$

Both bounds are positive and attained on $\partial D$. Let $T_\epsilon(z) = (1+\epsilon)(z-x)+x$ be the affine dilation of factor $(1+\epsilon)$ with $x$ fixed. Consider the curve $\Gamma$ given by the joining of the following three pieces:

(1) the line segment connecting $p$ to $T_\epsilon(p)$,

(2) the image $T_\epsilon(\Gamma_0)$, and

(3) the line segment connecting $T_\epsilon(q)$ to $q$.

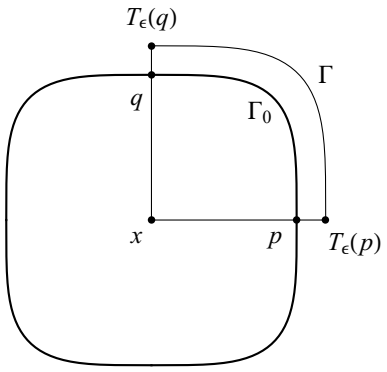


Figure 4.3. Alternative path integral near boundary

Let $\gamma\colon [0,\ell] \to \partial D$ be an arc-length parametrization of $\Gamma_0$ with $\gamma(0) = p$ and $\gamma(\ell) = q$. Then $|\gamma'(t)| = 1$ almost everywhere, and

$$\begin{aligned}
\left|\int_\Gamma f(z)\,dz - \int_{\Gamma_0} f(z)\,dz\right| &\le 2\epsilon MB + \left|\int_{T_\epsilon(\Gamma_0)} f(z)\,dz - \int_{\Gamma_0} f(z)\,dz\right| \\
&= 2\epsilon MB + \left|\int_0^\ell f(\gamma(t))\gamma'(t)\,dt - \int_0^\ell f(T_\epsilon(\gamma(t)))T_\epsilon'(\gamma(t))\gamma'(t)\,dt\right| \\
&\le 2\epsilon MB + \int_0^\ell |f(\gamma(t)) - (1+\epsilon)f(T_\epsilon(\gamma(t)))|\,dt \\
&\le 2\epsilon MB + \epsilon\ell B + \int_0^\ell |f(\gamma(t)) - f(T_\epsilon(\gamma(t)))|\,dt
\end{aligned}$$

Now as $\epsilon \to 0$, we have $2\epsilon MB + \epsilon\ell B \to 0$, and

$$\int_0^\ell |f(\gamma(t)) - f(T_\epsilon(\gamma(t)))|\,dt \to 0$$

by dominated convergence theorem. Therefore, we may integrate along the boundary. $\square$

PROOF OF LEMMA 4.3. Let $G_P\colon \mathbb{C} \to \mathbb{R}$ be the Green's function for $P$. It is the unique continuous function on $\mathbb{C}$ satisfying (1) $G_P \equiv 0$ on $P$, (2) $G_P(z) = \log|z| + \gamma + o(1)$ near $\infty$ for some constant $\gamma$, and (3) $G_P$ is harmonic on $\hat{\mathbb{C}} \setminus P$. Let $\rho_P$ be a metric on $\mathbb{C}$ given by

$$\rho_P = e^{-2G_P(z)}|dz|$$

Its curvature form $\omega_P = 2\Delta G_P$ indicates that the metric $\rho_P$ is flat away from $\partial P$, and the curvature distribution equals $4\pi$ times the harmonic measure of $P$ supported on $\partial P$.

Consider the holomorphic 1-form

$$\eta = \frac{1}{[\Phi^{-1}(z)]^2}\, dz$$

on the complement of $P$. Since the Green's function satisfies $G_P(z) = \log|\Phi^{-1}(z)|$ on $\hat{\mathbb{C}} \setminus P$, we see that $|\eta| = \rho_P$ on $\hat{\mathbb{C}} \setminus P$. Let $F\colon \hat{\mathbb{C}} \setminus P \to \mathbb{C}$ be defined by

$$F(z) = \int_\infty^z \frac{1}{[\Phi^{-1}(\zeta)]^2}\, d\zeta = \int_\infty^z \eta.$$

Then $\eta = dF = F^*(dz)$, where $dz$ is the standard holomorphic 1-form. Since $F^*|dz| = |\eta| = \rho_P$, which is the desired conformal metric on $\hat{\mathbb{C}}$, we conclude that $F$ is a Euclidean development of the harmonic cap $\hat{P}$ by $z \in \hat{\mathbb{C}} \setminus P$.

Now let $P$ be a Jordan domain with rectifiable boundary, and let $\Phi\colon \hat{\mathbb{C}} \setminus \overline{\mathbb{D}} \to \hat{\mathbb{C}} \setminus P$ be a conformal isomorphism fixing $\infty$. By Carathéodory's theorem, $\Phi$ continuously extends to a homeomorphism on $\partial\,\mathbb{D}$. By rectifiability of $\partial P$, there exists an arc-length parametrization $\gamma(t)$ of $\partial P$. In particular, $\gamma(t)$ is 1-Lipschitz. By Rademacher theorem,

the derivative $\gamma'(t)$ exists almost everywhere. Let $\hat{\gamma}(t) = F(\gamma(t))$. Then $\hat{\gamma}(t)$ parametrizes $\partial\hat{P}$. It would suffice to show $|\hat{\gamma}'(t)| = 1$ almost everywhere.

Let $a \in \mathbb{R}$ be a parameter such that $\gamma'(a)$ exists. Then $|\gamma'(a)| = 1$. Thus

$$\begin{aligned}
\frac{d}{dt}\hat{\gamma}(t)\bigg|_{t=a} &= \lim_{t\to a} \frac{\hat{\gamma}(t) - \hat{\gamma}(a)}{t-a} = \lim_{t\to a} \frac{F(\gamma(t)) - F(\gamma(a))}{t-a} \\
&= \lim_{t\to a} \frac{F(\gamma(t)) - F(\gamma(a))}{\gamma(t) - \gamma(a)} \frac{\gamma(t) - \gamma(a)}{t-a} \\
&= \gamma'(a) \lim_{t\to a} \frac{F(\gamma(t)) - F(\gamma(a))}{\gamma(t) - \gamma(a)} \\
&= \gamma'(a) \lim_{t\to a} \frac{1}{\gamma(t) - \gamma(a)} \int_{\gamma(a)}^{\gamma(t)} \frac{1}{[\Phi^{-1}(\zeta)]^2}\, d\zeta \\
&= \gamma'(a) \lim_{t\to a} \frac{1}{\gamma(t) - \gamma(a)} \int_{a}^{t} \frac{\gamma'(\tau)}{[\Phi^{-1}(\gamma(\tau))]^2}\, d\tau
\end{aligned}$$

The integral is taken along any path connecting $\gamma(a)$ to $\gamma(t)$ within the domain $\hat{\mathbb{C}} \setminus P$. By Lemma 4.4, we may take the integral along $\partial P$, which justifies the last equal sign.

It now suffices to show the limit in the expression above has norm 1. Let $\epsilon > 0$. Let $\delta > 0$ be small enough such that for all $x \in \partial P$ with $|x - \gamma(a)| < \delta$, we have

$$\left|[\Phi^{-1}(\gamma(a))]^2 - [\Phi^{-1}(x)]^2\right| < \epsilon.$$

Consider the limit for $t \in (a-\delta, a+\delta)$. Because $\gamma(t)$ is an arc-length parametrization, $|\gamma(t)-\gamma(a)| < \delta$. Then for almost every $\tau \in [a,t]$, we have $|\gamma'(\tau)| = 1$. Thus

$$\begin{aligned}\left|\int_a^t \frac{\gamma'(\tau)}{[\Phi^{-1}(\gamma(\tau))]^2}\,d\tau - \int_a^t \frac{\gamma'(a)}{[\Phi^{-1}(\gamma(a))]^2}\,d\tau\right| &\le \int_a^t \left|\frac{1}{[\Phi^{-1}(\gamma(\tau))]^2} - \frac{1}{[\Phi^{-1}(\gamma(a))]^2}\right| dt \\ &= \int_a^t \frac{|[\Phi^{-1}(\gamma(\tau))]^2 - [\Phi^{-1}(\gamma(a))]^2|}{|\Phi^{-1}(\gamma(\tau))|^2|\Phi^{-1}(\gamma(a))|^2}\,dt \\ &= \int_a^t \left|[\Phi^{-1}(\gamma(\tau))]^2 - [\Phi^{-1}(\gamma(a))]^2\right| dt \\ &< \epsilon|t-a|.\end{aligned}$$

However, the integrand in

$$\int_a^t \frac{\gamma'(a)}{[\Phi^{-1}(\gamma(a))]^2}\,d\tau$$

is constant with complex norm 1. Therefore,

$$(1-\epsilon)|t-a| < \left|\int_a^t \frac{\gamma'(\tau)}{[\Phi^{-1}(\gamma(\tau))]^2}\,d\tau\right| < (1-\epsilon)|t-a|$$

and

$$(1-\epsilon)\lim_{t\to a}\frac{|t-a|}{|\gamma(t)-\gamma(a)|} < \left|\lim_{t\to a}\frac{1}{\gamma(t)-\gamma(a)}\int_a^t \frac{\gamma'(\tau)}{[\Phi^{-1}(\gamma(\tau))]^2}\,d\tau\right| < (1+\epsilon)\lim_{t\to a}\frac{|t-a|}{|\gamma(t)-\gamma(a)|}$$

It follows that

$$1-\epsilon = \frac{1-\epsilon}{|\gamma'(a)|} < \left|\lim_{t\to a}\frac{1}{\gamma(t)-\gamma(a)}\int_a^t \frac{\gamma'(\tau)}{[\Phi^{-1}(\gamma(\tau))]^2}\,d\tau\right| < \frac{1+\epsilon}{|\gamma'(a)|} = 1+\epsilon.$$

for arbitrary $\epsilon > 0$. Hence, we have come to the conclusion that $|\hat{\gamma}'(a)| = |\gamma'(a)| = 1$. $\square$

Lemma 4.3 allows for perimeter gluing of $\partial P$ and $\partial \hat{P}$. To be more precise, let $\gamma\colon [0, L] \to \mathbb{C}$ be an arc-length parametrization of $\partial P$. Then the perimeter gluing is given by $\gamma(t) \sim F(\gamma(t))$. We are now ready to prove the theorem for Jordan domains with rectifiable boundary.

**Lemma 4.5.** *Let $P \subseteq \mathbb{C}$ be a Jordan domain with rectifiable boundary. If $P$ and its harmonic cap $\hat{P}$ differs by a reflection, then $P$ is a disk.*

Proof. Let $\Phi\colon \hat{\mathbb{C}} \setminus \overline{\mathbb{D}} \to \hat{\mathbb{C}} \setminus P$ be a conformal isomorphism fixing $\infty$. Let $\Psi\colon \mathbb{D} \to \hat{P}$ be defined by $\Psi = F \circ \Phi \circ c$, where $c\colon \mathbb{D} \to \hat{\mathbb{C}} \setminus \overline{\mathbb{D}}$ is the reflection across the unit circle given by $c(z) = 1/\overline{z}$, which fixes every point on the unit circle if extended. Notice that $\Psi$ is an antiholomorphic bijection that extends to a homeomorphism (which is orientation-reversing) on the boundary. Now assume that $P$ and $\hat{P}$ differs by a reflection, then there exists some appropriate reflection $r(z) = \omega\overline{z} + \zeta$, where $\omega \in \partial\,\mathbb{D}$ and $\zeta \in \mathbb{C}$, such that $r \circ \Psi\colon \mathbb{D} \to P$ is a holomorphic bijection that agrees with $\Phi$ on the boundary by perimeter gluing. So $\Phi$ and $r \circ \Psi$ together define a homeomorphism $h\colon \mathbb{C} \to \mathbb{C}$, which is holomorphic off the unit circle. Then $h$ is entire by Morera's Theorem. Because $h$ is injective, Liouville's Theorem further implies that $h$ is linear of the form $h(z) = \alpha z + \beta$, where $\alpha \neq 0$. Therefore, $P$ is necessarily a disk. □

Combining the result of Lemma 4.2 and 4.5, we have completed the proof of the "only if" part of Theorem 1.1.

CHAPTER 5

# Harmonic Planarity of Jordan Arcs

We have also seen in Example 3.3 that the harmonic cap of $[-2, 2]$ can be parametrized by the function $g\colon \mathbb{D} \to \mathbb{C}$ with

$$g(z) = z - \frac{z^3}{3}.$$

Because $\overline{g(z)} = g(\overline{z})$, the real axis is a reflection axis of symmetry. Perimeter gluing of $P$ and $\hat{P}$ would identify conjugating points on $\partial\hat{P}$ to the same point on the segment $P$, thus also resulting in a convex shape that is entirely contained in a plane. We see from the argument above that a line segment is harmonically planar. In fact, there is a whole family of harmonically planar Jordan arcs, namely, the circular arcs.

## 5.1. Circular Arcs Are Harmonically Planar

**Lemma 5.1.** *If $\Gamma \subseteq \mathbb{C}$ is a circular arc, then it is harmonically planar.*

We will prove this lemma in three steps: (1) construct the appropriate conformal isomorphism for an arbitrary circular arc, (2) find a criterion for the circular arcs to be harmonically planar, and (3) show that the criterion is met for all circular arcs.

Proof. We assume that $\Gamma$ is an arc of the unit circle with one endpoint sitting at $1 \in \partial\,\mathbb{D}$. The length of $\Gamma$ will be characterized by identifying each such circular arc with the image of a specific ray under a Möbius transformation. The following construction parameterizes the family of circular arcs by the real numbers $\mathbb{R}$.

Let $f\colon \mathbb{H} \to \mathbb{D}$ be the Möbius transformation

$$f(z) = \frac{z-i}{z+i}.$$

Then $f^{-1}\colon \mathbb{D} \to \mathbb{H}$ has the expression

$$f^{-1}(z) = i \cdot \frac{1+z}{1-z}.$$

Further, $f$ maps any ray of the form $(-\infty, a] \subseteq \mathbb{R}$ to a circular arc on the unit circle, and the length of the arc is uniquely determined by the value of $a \in \mathbb{R}$. Let $\Gamma_a$ be the circular arc given by the image of $(-\infty, a] \cup \{\infty\}$ under the Möbius transformation $f$. The following composition of functions gives a conformal isomorphism from $\hat{\mathbb{C}} \setminus \Gamma_a$ to $\hat{\mathbb{C}} \setminus \overline{\mathbb{D}}$.

$$\hat{\mathbb{C}} \setminus \Gamma_a \xrightarrow{f^{-1}} \mathbb{C} \setminus (-\infty, a] \xrightarrow{z-a} \mathbb{C} \setminus (-\infty, 0] \xrightarrow{z^{1/2}} -i\,\mathbb{H} \xrightarrow{g} -i\,\mathbb{H} \xrightarrow{1/f(iz)} \mathbb{C} \setminus \overline{\mathbb{D}}$$

where $f\colon \mathbb{H} \to \mathbb{D}$ is the Möbius transformation defined above, and $g\colon -i\,\mathbb{H} \to -i\,\mathbb{H}$ is an affine transformation of the right-half plane defined by

$$g(z) = \sqrt{2\big(a + \sqrt{a^2+1}\big)}\, z + \big(a + \sqrt{a^2+1}\big) i.$$

Under this sequence of compositions, the image of $\infty$ is $\infty$, as checked in the following sequence of images

$$\infty \xrightarrow{f^{-1}} -i \xrightarrow{z-a} -i - a \xrightarrow{z^{1/2}} (a^2+1)^{1/4} e^{i\theta/2} \xrightarrow{g} 1 \xrightarrow{1/f(iz)} \infty$$

where $cot(\theta) = a$ with $\theta \in (-\pi, 0)$. This completes step (1) of the proof.

Let $\gamma(t) = e^{it}$, $0 \le t \le \varphi$, where $e^{i\varphi} = f(a)$, be an arc-length parametrization of $\Gamma_a$. Then $s\colon [0, 2\varphi] \to \mathbb{C}$ given by

$$s(t) = \begin{cases} e^{it}, & \text{if } 0 \le t \le \varphi, \\ e^{i(2\varphi - t)}, & \text{if } \varphi \le t \le 2\varphi \end{cases}$$

is a counterclockwise arc-length parameterization of the outside of the planar shape $\Gamma_a$. Let $\Phi\colon \hat{\mathbb{C}} \setminus \overline{\mathbb{D}} \to \hat{\mathbb{C}} \setminus \Gamma_a$ be a conformal isomorphism that satisfies $\Phi(\infty) = \infty$ and $\Phi(1) = \gamma(0)$. Because $\Gamma_a$ is smooth, $\Phi$ continuously extend to $\hat{\mathbb{C}} \setminus \mathbb{D}$, and $\partial\mathbb{D}$ maps onto $\Gamma_a$ through the extension. Thus

$$\kappa(t) = 4\pi\mu(s[0,t]) = 2\Big[\arg\Big(\Phi^{-1}\big(s(t)\big)\Big)\Big],$$

where arg is the branch of the argument function taking $[0, 2\pi)$ as its range, is the cumulative curvature distribution along both sides of $\Gamma$, parameterized by arc length. By Equation 3.2, the boundary of the harmonic cap $\hat{\Gamma}_a$ has parametrization

$$\hat{s}(t) = \int_0^t e^{i(\alpha(x) - \kappa(x))}\, dx,$$

and thus

$$\hat{s}'(t) = e^{i(\alpha(t) - \kappa(t))}$$

Let $\Psi_1, \Psi_2\colon \hat{\mathbb{C}} \setminus \Gamma_a \to \hat{\mathbb{C}} \setminus \overline{\mathbb{D}}$ be the conformal isomorphisms defined in the aforementioned construction, where each of $\Psi_k$ takes a different branch of $z^{1/2}$ at the third function. Then $\Psi_1(z)$ and $\Psi_2(z)$ are indeed the inverse of $\Phi$ outside of $\Gamma$, and they give two different

preimages of $\Phi^{-1}(z)$ for $z \in \Gamma_a$. Therefore,

$$\begin{cases} \hat{s}'(t) = ie^{it} \cdot \left[\Psi_1(e^{it})\right]^{-2} \\ \hat{s}'(2\varphi - t) = -ie^{it} \cdot \left[\Psi_2(e^{it})\right]^{-2} \end{cases}$$

for $t < \varphi$. In order for $\Gamma_a$ to be harmonically planar, the harmonic cap $\hat{\Gamma}_a$ needs to have a reflection axis of symmetry, and perimeter gluing should identify symmetric points to the same point on $\Gamma_a$. With the given assumption, we have $\gamma'(0) = i$, thus implying $\hat{s}'(0) = i$ as well. From Figure 5.1, we see that the boundary of the harmonic cap $\hat{\Gamma}_a$ must satisfy the condition

$$\hat{s}'(t)\hat{s}'(2\varphi - t) = 1,$$

Or, equivalently,

$$(\star) \qquad e^{2it} = \left[\Psi_1(e^{it})\right]^2 \left[\Psi_2(e^{it})\right]^2.$$

Now we have completed step (2) of the proof.

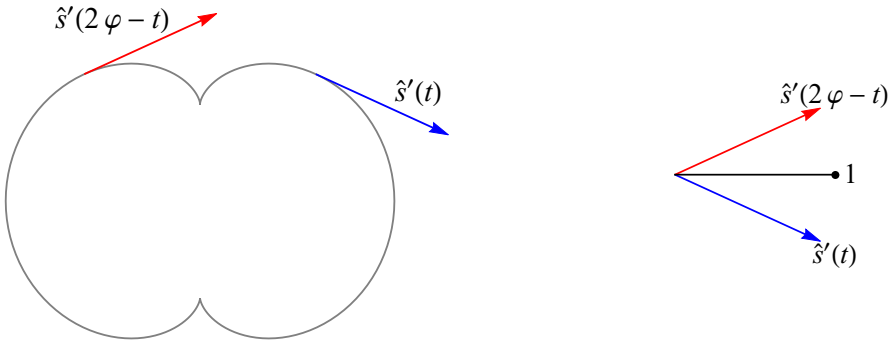


Figure 5.1. Harmonically planar Jordan arcs must have harmonic caps with reflection symmetry. The symmetry condition is represented by the relation between tangent vectors at the same distance away from $\hat{s}(0) = \hat{s}(2\varphi)$ along the boundary curve of $\hat{\Gamma}_a$.

To show condition $(\star)$ is satisfied by $\Gamma_a$, we conduct the following computation.

$$\begin{aligned}
f^{-1}\colon\ & e^{it} \mapsto -\cot(t/2) \\
z-a\colon\ & -\cot(t/2) \mapsto -\cot(t/2) - a \\
z^{1/2}\colon\ & -\cot(t/2) - a \mapsto \pm i\sqrt{\cot(t/2)+a} \\
g\colon\ & \pm i\sqrt{\cot(t/2)+a} \mapsto i\Big(a+\sqrt{a^2+1} \pm \sqrt{2\big(a+\sqrt{a^2+1}\big)\big(\cot(t/2)+a\big)}\Big) \\
\frac{1}{f(iz)} = \frac{z+1}{z-1}\colon\ & i\Big(a+\sqrt{a^2+1} \pm \sqrt{2\big(a+\sqrt{a^2+1}\big)\big(\cot(t/2)+a\big)}\Big) \\
& \mapsto \frac{-i+\Big(a+\sqrt{a^2+1} \pm \sqrt{2\big(a+\sqrt{a^2+1}\big)\big(\cot(t/2)+a\big)}\Big)}{i+\Big(a+\sqrt{a^2+1} \pm \sqrt{2\big(a+\sqrt{a^2+1}\big)\big(\cot(t/2)+a\big)}\Big)} =: \zeta_\pm
\end{aligned}$$

The values $\zeta_\pm$ are the preimages of $e^{it}$, and their product is

$$\zeta_+\zeta_- = \frac{\big(a+\sqrt{a^2+1}-i\big)^2 - 2\big(a+\sqrt{a^2+1}\big)\big(\cot(t/2)+a\big)}{\big(a+\sqrt{a^2+1}+i\big)^2 - 2\big(a+\sqrt{a^2+1}\big)\big(\cot(t/2)+a\big)}$$

The numerator and denominator of the product are complex conjugates of each other. Therefore, the argument of $\zeta_+\zeta_-$ is twice the argument of its numerator. To isolate the

numerator,

$$\begin{aligned}
\mathrm{Re}(\text{numerator}) &= 2a^2 + 2a\sqrt{a^2+1} - 2\big(a+\sqrt{a^2+1}\big)\big(\cot(t/2)+a\big) \\
&= 2a\big(a+\sqrt{a^2+1}\big) - 2\big(a+\sqrt{a^2+1}\big)\big(\cot(t/2)+a\big) \\
&= 2\big(a+\sqrt{a^2+1}\big)\big(a-\cot(t/2)-a\big) \\
&= -2\big(a+\sqrt{a^2+1}\big)\cot(t/2), \\
\mathrm{Im}(\text{numerator}) &= -2\big(a+\sqrt{a^2+1}\big).
\end{aligned}$$

Therefore,

$$\cot\Big[\arg(\text{numerator})\Big] = \frac{\mathrm{Re}(\text{numerator})}{\mathrm{Im}(\text{numerator})} = \cot(t/2).$$

It thus follows that $\arg(\zeta_+\zeta_-) = t$, and therefore, $\zeta_+^2\zeta_-^2 = e^{2it}$, which is precisely the symmetry condition ($\star$). □

Together with the harmonic cap computation of the line segment, we just completed the proof of Theorem 1.2.

**Theorem 1.2.** *If $\Gamma \subseteq \mathbb{C}$ is a line segment or a circular arc, then $\Gamma$ is harmonically planar.*

### 5.2. Are There Other Harmonically Planar Jordan Arcs?

We proved in Chapter 4 that a Jordan domain is harmonically planar if and only if it is a disk. We would desire a similar statement about Jordan arcs in the plane as planar shapes. Based on extensive numerical evidence, we conjecture that line segments and circular arcs are the only harmonically planar Jordan arcs.

**Conjecture.** *Let $\Gamma \subseteq \mathbb{C}$ be a Jordan arc. If $\Gamma$ is harmonically planar, then it is either a line segment or a circular arc.*

In order to attempt a proof, we first need to device an intrinsic property of the curve that leads to harmonic planarity, which we call the *symmetry assumption.*

**Lemma 1.3** (The Symmetry Assumption)**.** *Let $\Gamma \subseteq \mathbb{C}$ be a smooth Jordan arc, and let $\gamma\colon [0, L] \to \mathbb{C}$ be an arc-length parameterization of $\Gamma$, and assume that $\gamma(0) = 0$ and $\gamma'(0) = 1$. Let $\Phi\colon \hat{\mathbb{C}} \setminus \overline{\mathbb{D}} \to \hat{\mathbb{C}} \setminus \Gamma$ be a conformal isomorphism that fixes the point at $\infty$, and assume its continuous extension at the boundary satisfies $\Phi(1) = 0$. If $\Gamma$ is harmonically planar, then*

$$\gamma'(t) = \Phi_1^{-1}(\gamma(t)) \cdot \Phi_2^{-1}(\gamma(t)), \tag{1.1}$$

*where $\Phi_1^{-1}$ and $\Phi_2^{-1}$ are the two distinct branches of the inverse of $\Phi$ along $\Gamma$.*

Proof. Let $F\colon \hat{\mathbb{C}} \setminus \Gamma \to \mathbb{C}$ be the map given by

$$F(z) = \int_\infty^z \frac{1}{[\Phi^{-1}(w)]^2}\, dw$$

From the proof of Lemma 4.3, we know that the map $F$ is locally univalent, and its image is a Euclidean development of the harmonic cap $\hat{\Gamma}$. From its definition, we have

$$F'(z) = \frac{1}{[\Phi^{-1}(z)]^2}$$

Further, for $\zeta \in \Gamma$,

$$\lim_{z \to \zeta} F'(z) = \lim_{z \to \zeta} [\Phi^{-1}(z)]^{-2} \in S^1.$$

Thus $|F'(\zeta)| = 1$. If $\Gamma$ is a smooth curve, then by the chain rule, the only non-differentiable

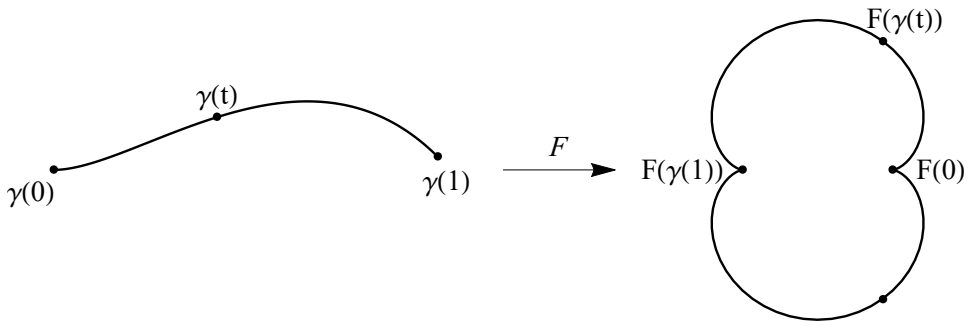


Figure 5.2. The symmetry assumption on Jordan arcs

points on $\partial\Gamma$ are the images of the endpoints. Further, the unit tangent vector at $F(\gamma(t))$ shown in the figure above is

$$\gamma'(t)F'(\gamma(t)) = \frac{\gamma'(t)}{[\Phi_1^{-1}(\gamma(t))]^2},$$

where $\Phi_1^{-1}$ takes inverse of $\gamma(t)$ approaching from above of the curve.

To assume the appropriate reflection axis of symmetry, we would need the unit tangent vector at the other image of $\gamma(t)$ to differ by a reflection. First, this unit tangent is

$$-\gamma'(t)F'(\gamma(t)) = \frac{-\gamma'(t)}{[\Phi_2^{-1}(\gamma(t))]^2},$$

where $\Phi_2^{-1}$ takes inverse of $\gamma(t)$ approaching from below of the curve. The symmetry condition would then require these two unit tangent vectors to be symmetric across the imaginary axis, hence

$$\frac{\gamma'(t)}{[\Phi_1^{-1}(\gamma(t))]^2} \cdot \frac{-\gamma'(t)}{[\Phi_2^{-1}(\gamma(t))]^2} = -1.$$

This simplifies to

$$\gamma'(t)^2 = [\Phi_1^{-1}(\gamma(t))]^2 \cdot [\Phi_2^{-1}(\gamma(t))]^2.$$

From the assumption $\Phi(1) = 0$, the symmetry assumption becomes

$$\gamma'(t) = \Phi_1^{-1}(\gamma(t)) \cdot \Phi_2^{-1}(\gamma(t)).$$

□

For a curve planar shape $\Gamma$, the conformal isomorphism $\Phi\colon \hat{\mathbb{C}}\setminus\overline{\mathbb{D}} \to \hat{\mathbb{C}}\setminus\Gamma$ fixing the point at $\infty$ defines a *conformal lamination* of the unit circle. To be more precise,

**Definition 5.2.** Given a curve $\Gamma$ and a conformal isomorphism $\Phi\colon \hat{\mathbb{C}}\setminus\overline{\mathbb{D}} \to \hat{\mathbb{C}}\setminus\Gamma$ fixing the point at $\infty$, the **conformal lamination** $L_c$ induced by $\Phi$ on the unit circle is an equivalence relation defined by

$$\xi \sim \eta \text{ if and only if } \Phi(\xi) = \Phi(\eta)$$

for $\xi, \eta \in \partial\,\mathbb{D}$.

Let $\varphi(t)$ and $\psi(t)$ be the two distinct pre-images of the arc-length parameterization $\gamma(t)$ of $\Gamma$, in the sense that

$$\Phi(\varphi(t)) = \Phi(\psi(t)) = \gamma(t).$$

Then we can recover the curve $\Gamma$ with the conformal map. In fact, we are able to recover any rectifiable curve, up to an affine transformation, with only the lamination information.

**Lemma 5.3.** *Let* $\Gamma$ *and* $\Gamma_0$ *be rectifiable Jordan arcs, and let* $\Phi\colon \hat{\mathbb{C}}\setminus\overline{\mathbb{D}} \to \hat{\mathbb{C}}\setminus\Gamma$ *and* $\Phi_0\colon \hat{\mathbb{C}}\setminus\overline{\mathbb{D}} \to \hat{\mathbb{C}}\setminus\Gamma_0$ *be their respective conformal isomorphisms fixing infinity. If the induced conformal laminations agree on the unit circle, then* $\Gamma_0$ *is an affine image of* $\Gamma$.

Proof. Consider the map $\Phi_0 \circ \Phi^{-1}\colon \hat{\mathbb{C}}\setminus\Gamma \to \hat{\mathbb{C}}\setminus\Gamma_0$. The map is conformal off $\Gamma$. Because the laminations agree, it is also continuous across $\Gamma$. A stronger form of Cauchy integral theorem [**2**] tells us that

$$\oint_C \Phi_0 \circ \Phi^{-1}(z)\, dz = 0$$

for all closed, positively-oriented rectifiable curves $C$. Thus $\Phi_0 \circ \Phi^{-1}$ is entire. Because it also fixes $\infty$, it must be an affine map. □

The symmetry assumption (1.1) relates the direction of the curve to the conformal angles by $\gamma'(t) = \varphi(t)\psi(t)$. This defines an alternative method to recover the original curve $\Gamma$, given that $\Gamma$ is harmonically planar, namely, we can recover

$$\gamma(t) = \int_0^t \varphi(x)\psi(x)\, dx.$$

The collection of all harmonically planar Jordan arcs is then all curves with agreeing recovery from both methods.

CHAPTER 6

# Schwarz-Christoffel Transformations and the Wedge Family

In this chapter, we investigate a powerful tool in computing conformal isomorphisms, the Schwarz-Christoffel transformations. The main reference for this chapter is [**9**] by Driscoll and Trefethen, while the MATLAB computation toolbox and its manual are available at [**7, 8**]. The MATLAB toolbox helps in generating a number of harmonic cap figures in the next two chapters. We conclude our study of Schwarz-Christoffel transformations by investigating the simplest family of polygonal lines, the wedge family $W_\theta$, in detail.

## 6.1. Schwarz-Christoffel Transformations

**6.1.1. The fundamental idea.** The idea behind the Schwarz-Christoffel transformation is that a conformal mapping $f$ may have a derivative that can be expressed as

$$f' = \prod f_k$$

for some canonical functions $f_k$. Geometrically, the significance of the assumption above is that

$$\arg f' = \sum \arg f_k$$

Restricted on $\mathbb{R}$, if each $\arg f_k$ on the right hand side is a step function, the resulting $\arg f'$ on the left is piecewise constant with specific jumps. In the classical setting, we

would have $f$ mapping the real axis to a polygon, and extend it to be a conformal map of the upper half plane $\mathbb{H}$ onto the interior of a polygon.

To be more concrete, let $P$ be the region in the complex plane $\mathbb{C}$ bounded by a polygon $\Gamma$ with vertices $w_1, \ldots, w_n$, given in counterclockwise order, and interior angles $\alpha_1\pi, \ldots, \alpha_n\pi$. Let $f$ be a conformal map from the upper half plane $\mathbb{H}$ onto $P$, and let $z_k = f^{-1}(w_k)$ be the $k$-th **prevertex**. Figure 6.1 demonstrates the schematic of Schwarz-Christoffel transformations together with these definitions.

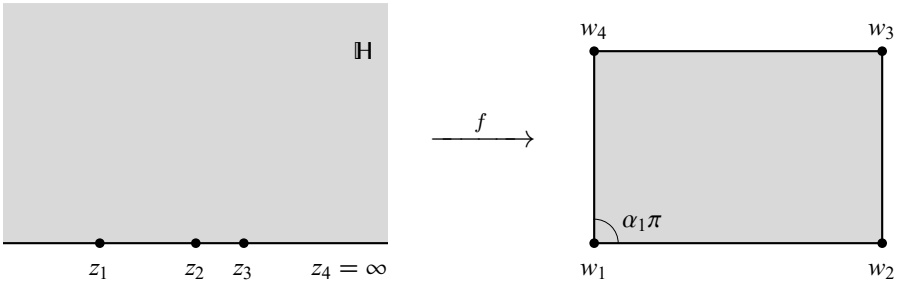


Figure 6.1. A schematic of Schwarz-Christoffel transformations

By the Schwarz reflection principle, $f$ can be analytically continued across the segment joining $z_k$ to $z_{k+1}$. In particular, $f'$ exists, and $\arg f'$ is constant on this segment. Furthermore, $\arg f'$ must undergo a specific jump at $z = z_k$:

$$\left[\arg f'(z)\right]_{z_k^-}^{z_k^+} = (1 - \alpha_k)\pi = \beta_k\pi \tag{6.1}$$

The angle $\beta_k\pi$ is the **turning angle** at the $k$-th vertex. A particular function that is analytic in $\mathbb{H}$, satisfies Equation 6.1, and otherwise has constant $\arg f'$ on $\mathbb{R}$ is

$$f_k(z) = (z - z_k)^{-\beta_k}$$

The preceding argument suggests the following *Fundamental Theorem of Schwarz-Christoffel Mapping.*

**Theorem 6.1** (Fundamental Theorem of Schwarz-Christoffel Mapping)**.** *Let $P$ be the interior of a polygon $\Gamma$ with vertices $w_1, \ldots, w_n$ and interior angles $\alpha_1\pi, \ldots, \alpha_n\pi$ in counterclockwise order. Let $f\colon \mathbb{H} \to P$ be a conformal map. Then*

$$f(z) = A + C \int^z \prod_{k=1}^{n} (\zeta - z_k)^{\alpha_k - 1}\, d\zeta \tag{6.2}$$

*for some complex constants $A$ and $C$, where $w_k = f(z_k)$ for all $k = 1, \ldots, n$.*

An outline of the proof can be found in [**9**]. We include a detailed proof here for the purpose of completeness.

Proof. Without loss of generality, assume all prevertices $z_k$ are finite.

By Schwarz reflection principle, the function $f$ can be analytically continued to the lower half plane; the image of the continuation is the reflection of $P$ along one side of $\Gamma$. By reflecting again about a side of the new polygon, we return analytically to the upper half plane. This can be done for any even number of reflections of $P$, each giving a branch of $f$. The image of each branch is a translated and rotated copy of $P$. Thus $f''/f'$ is an invariant among these branches because

$$\frac{[A + Cf(z)]''}{[A + Cf(z)]'} = \frac{f''(z)}{f'(z)}.$$

Therefore, $f''(z)/f'(z)$ can be defined as a single-valued analytic function everywhere in the closed upper half plane, except at the prevertices $z_k$. Similarly, odd numbers of

reflections define $f''(z)/f'(z)$ as a single-valued analytic function in the closed lower half plane, except at the prevertices $z_k$.

Now we look at the prevertices $z_k$. Locally, $f(z) = (z - z_k)^{\alpha_k}$ in some coordinates. Thus

$$f'(z) = (z - z_k)^{\alpha_k - 1}\psi(z)$$

for some function $\psi$ analytic in a neighborhood of $z_k$. Therefore, $f''(z)/f'(z)$ has a simple pole at $z_k$ with residue $\alpha_k - 1$, and therefore, the function

$$h(z) = \frac{f''(z)}{f'(z)} - \sum_{k=1}^{n} \frac{\alpha_k - 1}{z - z_k}$$

removes all the simple poles and is an entire function.

Because prevertices are finite, $f$ is analytic at $\infty$ (evaluates to some point on one side of the polygon). Thus the function $f(1/z)$ could be given by a Taylor series

$$f(1/z) = c_0 + \sum_{k=1}^{\infty} c_k z^k$$

near $z = 0$. The Laurent expansion of $f(z)$ at $\infty$ is then

$$f(z) = c_0 + \sum_{k=1}^{\infty} c_k z^{-k}$$

It then follows that

$$\lim_{z\to\infty} \frac{f''(z)}{f'(z)} = 0$$

Thus $h(z) \to 0$ as $z \to \infty$. By Liouville's Theorem, $h(z) \equiv 0$.

Now we have established that

$$\frac{f''(z)}{f'(z)} = \sum_{k=1}^{n} \frac{\alpha_k - 1}{z - z_k}. \tag{6.3}$$

Notice that

$$\frac{d}{dz} \log(f'(z)) = \frac{f''(z)}{f'(z)} = \sum_{k=1}^{n} \frac{\alpha_k - 1}{z - z_k}.$$

Integrating twice, and we get the Schwarz-Christoffel formula in Equation 6.2. □

**6.1.2. Schwarz-Christoffel exterior maps.** A few variations of the Schwarz-Christoffel formula allows us to map simply connected domains in $\mathbb{C}$ to polygons [**9**]. Of all these variations, the mapping formula from the disk to the exterior region of a polygon is the most useful for our context.

**Theorem 6.2.** *Let $P$ be the region exterior to a bounded polygon $\Gamma$, where $w_1, \ldots, w_n$ are the vertices of $\Gamma$ in the **clockwise** direction, and $\alpha_1\pi, \ldots, \alpha_n\pi$ are the **interior** angles of the polygon at respective vertices. Let $f\colon \mathbb{D} \to \hat{\mathbb{C}} \setminus P$ be a conformal isomorphism that maps $0$ to $\infty$. Then*

$$f(z) = A + C \int^{z} \zeta^{-2} \prod_{k=1}^{n} \left(1 - \frac{\zeta}{z_k}\right)^{1-\alpha_k} d\zeta \tag{6.4}$$

*for some complex constants $A$ and $C$, where $f(z_k) = w_k$.*

Equation 6.4 helps us construct the Riemann map explicitly for the region exterior to a polygon. Furthermore, because $f(0) = \infty$, the pushforward $f_*\lambda$, where $\lambda$ is the normalized arclength measure on $\partial\,\mathbb{D}$, is precisely the harmonic measure of the polygon.

## 6.2. The Wedge Family

We are particularly interested in the family of wedges as planar shapes. To be precise, a **wedge** is a planar shape consisting of two equal-length line segments joined at one endpoint at an angle. A canonical model of this planar shape is

$$W_\theta = \{z \in \mathbb{C} \mid z = re^{i\alpha\pi} \text{ where } r \in [0,1] \text{ and } \alpha = 0 \text{ or } \theta\}.$$

for $\theta \in (0,1]$. We use the Schwarz-Christoffel exterior formula to find a conformal isomorphism between $\mathbb{D}$ and $\hat{\mathbb{C}} \setminus W_\theta$. Because such a conformal mapping is unique up to rotation, and because of the symmetry of $W_\theta$, we may assume the following table of parameters for the SC exterior map.

| $k$ | $w_k$ | $\alpha_k$ | $z_k$ |
|---|---|---|---|
| 1 | 0 | $2-\theta$ | 1 |
| 2 | 1 | 0 | $\omega$ |
| 3 | 0 | $\theta$ | $-1$ |
| 4 | $e^{i\theta\pi}$ | 0 | $\omega^{-1}$ |

The Carathéodory theorem guarantees a continuous extension of $f$ to $\overline{\mathbb{D}}$, so the prevertices $z_k$ are well-defined. Figure 6.2 is a schematic of the conformal mapping $f\colon \mathbb{D} \to \hat{\mathbb{C}} \setminus W_\theta$ as described in Theorem 6.2.

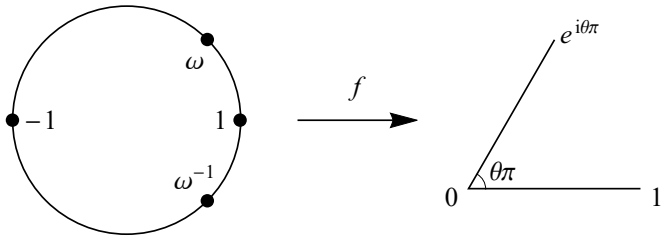


Figure 6.2. A schematic of the conformal mapping $f\colon \mathbb{D} \to \hat{\mathbb{C}} \setminus W_\theta$

The value of $\omega \in S^1$ is not arbitrary. For every $\theta \in (0, 1]$, there exists a unique $\omega \in S^1$ such that $f$ is indeed a conformal isomorphism, as demonstrated in the following lemma.

**Lemma 6.3** (Arccosine Relation)**.** *For every $\theta \in (0, 1]$, $f$ as described by Equation 6.4 is a conformal isomorphism if and only if $\omega = (1 - \theta) + i\sqrt{1 - (1 - \theta)^2}$. An equivalent condition is* $\arg(\omega) = \cos^{-1}(\theta)$.

PROOF. In order for $f$ to be a conformal isomorphism, it is necessary that $f(1) = f(-1)$. Because $f$ is given in the form of a path integral, this would mean

$$\int_S f'(\zeta)\, d\zeta = 0, \tag{6.5}$$

where $S$ is the semicircular arc joining 1 to $-1$, and

$$\begin{aligned} f'(\zeta) &= C \cdot \zeta^{-2} \prod_{k=1}^{4} \Big(1 - \frac{\zeta}{z_k}\Big)^{1-\alpha_k} \\ &= C \cdot \zeta^{-2}(1 - \zeta)^{\theta-1}(1 - \omega^{-1}\zeta)(1 + \zeta)^{1-\theta}(1 - \omega\zeta) \\ &= C \cdot \zeta^{-2}\Big(\frac{1 - \zeta}{1 + \zeta}\Big)^{\theta-1}(1 - \omega^{-1}\zeta)(1 - \omega\zeta) \end{aligned}$$

The derivative $f'$ is defined everywhere on $S$ except possibly at $\omega$ and $\pm 1$. In this case where $0 < \theta \leq 1$, it is defined everywhere on the semicircular arc $S$ except at 1.

Let $\gamma(t) = e^{it}$ for $t \in [0, \pi]$. Then $\gamma$ parametrizes the semicircular arc $S$. Now Equation 6.5 becomes

$$\int_0^{\pi} \frac{d}{dt} f\big(\gamma(t)\big)\, dt = 0. \tag{6.6}$$

Let $\varphi = \operatorname{Arg}(\omega)$, and let $C$ absorb any non-zero complex constants that arise from the computation. Then

$$\begin{aligned}
\frac{d}{dt} f\big(\gamma(t)\big) &= \gamma'(t) \cdot f'\big(\gamma(t)\big) \\
&= ie^{it} \cdot Ce^{-2it} \left(\frac{1 - e^{it}}{1 + e^{it}}\right)^{\theta-1} (1 - e^{i(t-\varphi)})(1 - e^{i(t+\varphi)}) \\
&= Ce^{-it} \left(\frac{e^{-it/2} - e^{it/2}}{e^{-it/2} + e^{it/2}}\right)^{\theta-1} \cdot \frac{e^{-i(t-\varphi)/2} - e^{i(t-\varphi)/2}}{e^{-i(t-\varphi)/2}} \cdot \frac{e^{-i(t+\varphi)/2} - e^{i(t+\varphi)/2}}{e^{-i(t+\varphi)/2}} \\
&= Ce^{-it} \big(-i \tan(t/2)\big)^{\theta-1} \cdot e^{it} \cdot (-2i) \sin\left(\frac{t-\varphi}{2}\right) \cdot (-2i) \sin\left(\frac{t+\varphi}{2}\right) \\
&= C\big(\tan(t/2)\big)^{\theta-1} \sin\left(\frac{t-\varphi}{2}\right) \sin\left(\frac{t+\varphi}{2}\right) \\
&= C\big(\tan(t/2)\big)^{\theta-1} \big(\cos(\varphi) - \cos(t)\big) \\
&= C\big(\tan(t/2)\big)^{\theta-1} \big(\operatorname{Re}(\omega) - \cos(t)\big).
\end{aligned}$$

Thus the isomorphism condition stated in Equations 6.5 and 6.6 has been reduced to the problem of finding the correct value of $\operatorname{Re}(\omega)$ such that the definite integral

$$\int_0^\pi \big(\tan(t/2)\big)^{\theta-1} \big(\operatorname{Re}(\omega) - \cos(t)\big)\, dt = 0. \tag{6.7}$$

If $\theta \in (0, 1)$, then

$$\frac{d}{dt}\big(\tan(t/2)\big)^{\theta} = \frac{1}{2} \cdot \big(\cos(t/2)\big)^{-2} \cdot \theta \big(\tan(t/2)\big)^{\theta-1}.$$

Thus

$$\int \theta\big(\tan(t/2)\big)^{\theta-1}\, dt = \int 2\big(\cos(t/2)\big)^{2} \cdot \frac{d}{dt}\big(\tan(t/2)\big)^{\theta}\, dt.$$

Integrate the right hand side by parts,

$$\begin{aligned}\int \theta\big(\tan(t/2)\big)^{\theta-1}\,dt &= 2\big(\cos(t/2)\big)^2\cdot\big(\tan(t/2)\big)^{\theta} + \int \big(\tan(t/2)\big)^{\theta}\cdot 2\sin(t/2)\cos(t/2)\,dt \\ &= 2\cos(t/2)^2\tan(t/2)^{\theta} + 2\int \tan(t/2)^{\theta-1}\sin(t/2)^2\,dt \\ &= 2\cos(t/2)^2\tan(t/2)^{\theta} + \int \tan(t/2)^{\theta-1}\big(1-\cos(t)\big)\,dt.\end{aligned}$$

It then follows that the indefinite integral from Equation 6.7 is

$$\begin{aligned}&\int \big(\tan(t/2)\big)^{\theta-1}\big(\operatorname{Re}(\omega)-\cos(t)\big)\,dt \\ =&\int \tan(t/2)^{\theta-1}\big(1-\cos(t)\big)\,dt + \int \tan(t/2)^{\theta-1}\big(\operatorname{Re}(\omega)-1\big)\,dt \\ =&-2\cos(t/2)^2\tan(t/2)^{\theta} + \int \theta\tan(t/2)^{\theta-1}\,dt + \int \tan(t/2)^{\theta-1}\big(\operatorname{Re}(\omega)-1\big)\,dt \\ =&-2\cos(t/2)^2\tan(t/2)^{\theta} + \big(\theta+\operatorname{Re}(\omega)-1\big)\int \tan(t/2)^{\theta-1}\,dt.\end{aligned}$$

Evaluate the definite integral in Equation 6.7,

$$\begin{aligned}&\int_0^{\pi} \big(\tan(t/2)\big)^{\theta-1}\big(\operatorname{Re}(\omega)-\cos(t)\big)\,dt \\ =&\Big[-2\cos(t/2)^2\tan(t/2)^{\theta}\Big]_0^{\pi} + \big(\theta+\operatorname{Re}(\omega)-1\big)\int_0^{\pi}\tan(t/2)^{\theta-1}\,dt \\ =&-2\Big[\sin(t/2)^{\theta}\cos(t/2)^{2-\theta}\Big]_0^{\pi} + \big(\theta+\operatorname{Re}(\omega)-1\big)\int_0^{\pi}\tan(t/2)^{\theta-1}\,dt \\ =&\big(\theta+\operatorname{Re}(\omega)-1\big)\int_0^{\pi}\tan(t/2)^{\theta-1}\,dt.\end{aligned}$$

However, $\tan(t/2) > 0$ for all $t \in (0, \pi)$, thus the definite integral

$$\int_0^\pi \tan(t/2)^{\theta-1}\, dt > 0.$$

To enforce the isomorphism condition of Equation 6.7, we must have $\theta + \mathrm{Re}(\omega) - 1 = 0$. Therefore, $\mathrm{Re}(\omega) = 1 - \theta$. Because $\omega \in \partial\,\mathbb{D} \cap \mathbb{H}$, it follows that

$$\omega = (1-\theta) + i\sqrt{1-(1-\theta)^2}.$$

If $\theta = 1$, then $W_\theta$ is the line segment $[-1, 1]$ contained in the real axis. We know a conformal mapping $f\colon \mathbb{D} \to \hat{\mathbb{C}} \setminus [-1, 1]$ given by the formula $f(z) = -i(z - z^{-1})/2$. When $\omega = i$, the map $f$ satisfies the assumptions given by the table of prevertices and that $f(0) = \infty$. □

The image of the arc length parameterization $\gamma(t)$ of the unit semicircular arc $S$ under the conformal map $f_\theta\colon \mathbb{D} \to \hat{\mathbb{C}} \setminus W_\theta$ gives a parametrization of $W_\theta$ by harmonic measure. We first pick the appropriate complex constants $A$ and $C$ such that $f(\gamma(0)) = f(\gamma(\pi)) = 0$ and $f(\gamma(\varphi)) = 1$. Because

$$f(\gamma(t)) = A + C\int_0^t \tan(x/2)^{\theta-1}\big(1 - \theta - \cos(x)\big)\, dx,$$

we would need $A = 0$ for $f(\gamma(0)) = 0$. From the computation above, we know that

$$f(\gamma(t)) = C\int_0^t \tan(x/2)^{\theta-1}\big(1 - \theta - \cos(x)\big)\, dx = -2C\sin(t/2)^\theta \cos(t/2)^{2-\theta}$$

We know further that $f(\gamma(t))$ is real-valued, and it has a critical point at $\varphi = \arccos(1-\theta)$, whose critical value is the endpoint 1 of $W_\theta$ on the real axis. Therefore,

$$\begin{aligned} C &= -\frac{\sin(\varphi/2)^{-\theta}\cos(\varphi/2)^{\theta-2}}{2} \\ &= -\frac{1}{2}\left[\frac{1-\cos(\varphi)}{2}\right]^{-\theta/2}\left[\frac{1+\cos(\varphi)}{2}\right]^{\theta/2-1} \\ &= -\big[1-\cos(\varphi)\big]^{-\theta/2}\big[1+\cos(\varphi)\big]^{\theta/2-1} \\ &= -\theta^{-\theta/2}(2-\theta)^{\theta/2-1}. \end{aligned}$$

These combine to give

$$F_\theta(t) = f(\gamma(t)) = 2\theta^{-\theta/2}(2-\theta)^{\theta/2-1}\sin(t/2)^\theta\cos(t/2)^{2-\theta} \tag{1.3}$$

for $t \in [0,\pi]$, as a parametrization of both sides of the line segment $[0,1]$ by the harmonic measure of $W_\theta$, *i.e.*,

$$\mu_\theta(F_\theta([0,t])) = \frac{t}{2\pi}$$

for all $t \in [0,\pi]$. The harmonic measure parametrization of the other line segment of $W_\theta$ can be found by symmetry. Hence, we have just proved Theorem 1.4:

**Theorem 1.4.** *A Schwarz-Christoffel exterior map* $f\colon \mathbb{D} \to \hat{\mathbb{C}}\setminus W_\theta$ *is given by*

$$f(z) = C\int_0^z \zeta^{-2}\Big(\frac{1-\zeta}{1+\zeta}\Big)^{\theta-1}(1-\omega^{-1}\zeta)(1-\omega\zeta)\,d\zeta, \tag{1.2}$$

*where* $\omega = (1-\theta)+i\sqrt{1-(1-\theta)^2}$, *and* $C = -\theta^{-\theta/2}(2-\theta)^{\theta/2-1}$. *Furthermore,* $W_\theta \cap [0,1]$ *can be parametrized by harmonic measure with respect to conformal angle* $t \in [0,\pi]$ *as*

$$F_\theta(t) = f(\gamma(t)) = 2\theta^{-\theta/2}(2-\theta)^{\theta/2-1}\sin(t/2)^\theta \cos(t/2)^{2-\theta}. \tag{1.3}$$

*The parametrization of* $W_\theta \cap e^{i\theta\pi}[0,1]$ *can be described by symmetry.*

### 6.3. $W_\theta$ Is Not Harmonically Planar

The reflection symmetry of $W_\theta$ indicates that its harmonic measure $\mu_\theta$ is symmetrically distributed on its two consisting line segments, *i.e.*, for any measurable $E \subseteq [0,1]$, we have $\mu_\theta(E) = \mu_\theta(e^{i\theta\pi}E)$. Specifically, if

$$s(t) = \begin{cases} t, & \text{if } 0 \le t \le 1, \\ 2-t, & \text{if } 1 \le t \le 2, \\ e^{i\theta\pi}(t-2), & \text{if } 2 \le t \le 3, \\ e^{i\theta\pi}(4-t), & \text{if } 3 \le t \le 4. \end{cases}$$

is the arc-length parametrization of $W_\theta$, then

$$\mu_\theta(s[0,t]) = \mu_\theta(s[4-t,4]) = 1 - \mu_\theta(s[0,4-t]).$$

Equation 3.2 gives the curvature on the boundary of $\hat{W}_\theta$ by

$$|\hat{s}''(t)| = |-i\kappa'(t)e^{-i\kappa(t)}| = |\kappa'(t)|$$

where $t \notin \mathbb{Z}$ and $\kappa(t) = 4\pi\mu_\theta(s[0,t])$. Thus $|\hat{s}''(t)| = |\hat{s}''(4-t)|$ for $t \notin \mathbb{Z}$. This gives a reflection axis of symmetry of $\hat{W}_\theta$ by the line joining $\hat{s}(0)$ and $\hat{s}(2)$. However, because

$s(0) = s(2)$, perimeter gluing will identify $\hat{s}(0)$ with $\hat{s}(2)$ to form the boundary surface of the associated convex body. If we can show that the curvature on the boundary of $\hat{W}_\theta$ near $\hat{s}(0)$ and $\hat{s}(2)$ are different, we can then conclude that the associated convex body cannot be isometrically embedded into a planar region.

**Lemma 6.4.** $\lim_{\delta\to 0} |\hat{s}''(\delta)| \neq \lim_{\delta\to 0} |\hat{s}''(2-\delta)|$ *if* $\theta < 1$.

Proof. First of all, we recall from Chapter 2 that

$$\hat{s}(t) = \int_0^t e^{i(\alpha(x)-\kappa(x))} dx,$$

where $\kappa(t) = 4\pi\mu(s[0,t])$. By the fundamental theorem of calculus,

$$\hat{s}'(t) = e^{i(\alpha(t)-\kappa(t))}, \quad \text{and} \quad \hat{s}''(t) = i(\alpha'(t) - \kappa'(t))e^{i(\alpha(t)-\kappa(t))}.$$

Thus $|\hat{s}''(t)| = |\alpha'(t) - \kappa'(t)|$. We notice that

$$\kappa(F_\theta(t)) = 4\pi\mu_\theta\big(s\big([0, F_\theta(t)]\big)\big) = 4\pi\mu_\theta\big(F_\theta\big([0,t]\big)\big) = 4\pi \cdot \frac{t}{2\pi} = 2t.$$

Further, $F_\theta(0) = F_\theta(\pi) = 0 = s(0) = s(2)$, and $F_\theta$ is differentiable on $(0,\pi)$ with a single critical point whose critical value is 1. Thus $F_\theta$ is locally invertible near 0 and $\pi$, and its inverse is $\kappa/2$. It then follows that

$$\lim_{\delta\to 0} |\kappa'(\delta)| = \lim_{\epsilon\to 0} \frac{2}{|F'_\theta(\epsilon)|};$$
$$\lim_{\delta\to 0} |\kappa'(2-\delta)| = \lim_{\epsilon\to 0} \frac{2}{|F'_\theta(\pi-\epsilon)|}.$$

It now remains to compute $F'_\theta$. Let $C_\theta = 2\theta^{-\theta/2}(2-\theta)^{\theta/2-1}$, then

$$\begin{aligned}
F'_\theta(t) &= C_\theta \cdot \Big[\frac{\theta}{2} \cdot \sin(t/2)^{\theta-1}\cos(t/2)^{3-\theta} - \frac{2-\theta}{2} \cdot \sin(t/2)^{\theta+1}\cos(t/2)^{1-\theta}\Big] \\
&= \frac{C_\theta}{2} \cdot \Big[\theta \sin(t/2)^{\theta-1}\cos(t/2)^{3-\theta} + \theta \sin(t/2)^{\theta+1}\cos(t/2)^{1-\theta} \\
&\qquad\qquad - 2\sin(t/2)^{\theta+1}\cos(t/2)^{1-\theta}\Big] \\
&= \frac{C_\theta}{2} \cdot \Big[\theta \sin(t/2)^{\theta-1}\cos(t/2)^{1-\theta}\big(\cos(t/2)^2 + \sin(t/2)^2\big) - 2\sin(t/2)^{\theta+1}\cos(t/2)^{1-\theta}\Big] \\
&= \frac{C_\theta}{2} \cdot \Big[\theta - 2\sin^2(t/2)\Big]\cot(t/2)^{1-\theta}.
\end{aligned}$$

Because $\theta < 1$,

$$\begin{aligned}
\lim_{t\to 0} F'_\theta(t) &= \frac{\theta C_\theta}{2} \cdot \lim_{t\to 0} \cot(t/2)^{1-\theta} = \infty; \\
\lim_{t\to \pi} F'_\theta(t) &= \frac{(\theta-2) C_\theta}{2} \cdot \lim_{t\to \pi} \cot(t/2)^{1-\theta} = 0.
\end{aligned}$$

Lastly, recall that $\alpha(t)$ satisfies

$$s(t) = \int_0^t e^{i\alpha(x)}dx.$$

Thus $\alpha$ is locally constant near 0 and 1 on the wedge $W_\theta$, and $\alpha'(t) = 0$ It follows that Hence, we have $\lim_{\delta\to 0} |\hat{s}''(\delta)| \neq \lim_{\delta\to 0} |\hat{s}''(2-\delta)|$. □

The following claim is therefore immediate.

**Theorem 6.5.** *$W_\theta$ is not harmonically planar if $\theta \neq 1$.*

Alternatively, we can argue that $W_\theta$ does not satisfy the symmetry assumption in Equation 1.1 unless $\theta = 1$. Let $\gamma(t)$ be an arc-length parameterization of $W_\theta$. Assume

that $\gamma'(0) = 1$. Then $\gamma'(t) = 1$ for all $t \in (0, 1)$. Imposing the symmetry assumption, we would have

$$\Phi_1^{-1}(\gamma(t)) \cdot \Phi_2^{-1}(\gamma(t)) = 1$$

for all $t \in (0, 1)$. This would imply that the harmonic measures along both sides of the first edge equal, so the total harmonic measure on either side of the $W_\theta$ is $1/2$. From Proposition 6.3, this could only happen when $\theta = 1$.

When $\theta = 1$, the wedge $W_1$ is simply the line segment $[-1, 1]$ on the real axis. As we have observed in Chapter 5, we know that $W_1$ is harmonically planar.

In the next chapter, we will take a detailed investigation on the convex body associated to $W_\theta$ when $\theta = 1/2$. We will demonstrate that it consists of one flat face and three curved faces with numerical analysis based on data obtained from the MATLAB toolbox by Driscoll.

CHAPTER 7

# Numerical Algorithms for Harmonic Cap Developments

## 7.1. Turning Angle and Curvature

Given a polygon $P$ in $\mathbb{R}^2$ and a discrete non-negative probability measure $\mu$ supported on its vertices, is it possible to find another polygon $\hat{P}_\mu$ in $\mathbb{R}^2$ such that $P$ and $\hat{P}_\mu$ could glue together to form a polyhedron with curvature distribution $4\pi\mu$ on $\partial P \sim \partial \hat{P}_\mu$? If the answer to this question is yes, what shape would the resulting polyhedron in $\mathbb{R}^3$ have?

To address the first question, suppose that $P$ is an $n$-sided polygon with vertices $v_1, v_2, \ldots, v_n$ listed in counterclockwise orientation. With this information, the polygon $P$ is uniquely determined, and its side lengths $\ell_k$ and internal angles $\theta_k$ can all be computed from the location of the vertices. For simplicity, let $\theta_k$ be the internal angle of $P$ at the vertex $v_k$. Then the sum of external angles $\pi - \theta_k$ needs to be $2\pi$, *i.e.*,

$$\sum_{k=1}^{n} (\pi - \theta_k) = 2\pi.$$

Now suppose that the given probability measure $\mu$ charges the vertex $v_k$ with a mass $m_k$. Then $0 < m_k < 1$ and

$$\sum_{k=1}^{n} m_k = 1.$$

Now we assume that the polygon $\hat{P}_\mu$ were to exist, with vertices $\hat{v}_1, \hat{v}_2, \ldots, \hat{v}_n$ listed in clockwise orientation so that the gluing of the two polygons identifies each pair of vertices $(v_k, \hat{v}_k)$ and the corresponding edges between vertices, then, similar with $P$, the sum of

external angles $\pi - \hat{\theta}_k$ at vertex $\hat{v}_k$ needs to be $2\pi$, *i.e.*,

$$\sum_{k=1}^{n}(\pi - \hat{\theta}_k) = 2\pi.$$

Further, if we glue two polygons at their respective vertices $v_k$ and $\hat{v}_k$ with internal angles $\theta_k$ and $\hat{\theta}_k$, as illustrated in Figure 7.1. If the polyhedron is flat at the glued vertex $v_k$, the

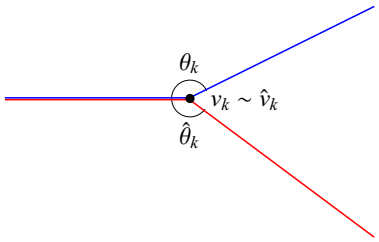


Figure 7.1. Angular defect at identified vertex

internal angles satisfy

$$\theta_k + \hat{\theta}_k = 2\pi.$$

When this equality is not satisfied, the discrepancy

$$\kappa(v_k) = 2\pi - \theta_k - \hat{\theta}_k$$

is the curvature concentrated at the glued vertex $v_k$. Under the assumption that $\hat{P}_\mu$ exists, the curvature distribution at the vertices is proportional to the given probability measure $\mu$, *i.e.*,

$$4\pi\mu(v_k) = \kappa(v_k) = 2\pi - \theta_k - \hat{\theta}_k.$$

With this information, we are able to construct the polygon $\hat{P}_\mu$ from the information of the polygon $P$ by an algorithm described as follows.

## 7.2. The Cap Construction Algorithm

The cap construction algorithm is described below as a series of functions implemented in Mathematica.

**7.2.1.** `CompanionShape[GivenPolygon,GivenCurvature].` This function takes in a list of complex numbers, representing the vertices of $P$ in counterclockwise order, together with corresponding curvature data at each vertex, and returns a list of complex numbers that *potentially* traces out the vertices of the polygon $\hat{P}_\mu$ in clockwise order. Note that if the polygon $\hat{P}_\mu$ of our context does not exist, this algorithm would return a polygonal line that does not form a Jordan curve. Details of this scenario will be discussed at the end of this section. The algorithm is implemented by the following steps.

(1) Check for incorrect inputs on the lists `GivenPolygon` and `GivenCurvature`.

(2) Compute the list of sides $s_k$ as complex vectors from the list of vertices $v_k$ specified by `GivenPolygon`.

(3) Compute the list of side lengths $\ell_k$ and internal angles $\theta_k$ from the list of vertices $v_k$ specified by `GivenPolygon`.

(4) Use the relation $\kappa(v_k) = 2\pi - \theta_k - \hat{\theta}_k$ to find the internal angles $\hat{\theta}_k$ of the candidate polygonal line for $\hat{P}_\mu$.

(5) The sides of the new polygon $\hat{P}_\mu$ shall have the same lengths as the sides of the original polygon $P$, but in opposite orientation. Therefore, using the list of side lengths $\ell_k$ and the list of new internal angles $\hat{\theta}_k$, we can compute the list of new sides $\hat{s}_k$ as complex vectors.

(6) The output `NewPolygonalLine` is a list of complex numbers obtained by sequentially adding the complex vectors $\hat{s}_k$ to the identified first vertex $v_1 \sim \hat{v}_1$. The first two vertices, $\hat{v}_1$ and $\hat{v}_2$, in `NewPolygonalLine` shall agree with the first two vertices, $v_1$ and $v_2$, in `GivenPolygon`. The length of the list `NewPolygonalLine` is one more than the length of `GivenPolygon`.

**7.2.2.** `CompanionShape[GivenPolygon].` When the curvature data is not specified, this function assumes uniformly distributed curvature on all of the vertices $v_k$ specified by `GivenPolygon`.

**7.2.3.** `DrawCompanionShapes[GivenPolygon,GivenCurvature].` This function calls the function `CompanionShape` with the given inputs, and produces the graphics of the original polygon $P$ together with the polygonal line representing the candidate boundary of the polygon $\hat{P}_\mu$, identifying the first two vertices of both $P$ and $\hat{P}_\mu$.

**7.2.4.** `DrawCompanionShapes[GivenPolygon].` When the curvature data is not specified, this function assumes uniformly distributed curvature on all of the vertices $v_k$ specified by `GivenPolygon`.

**7.2.5. Examples.** The followings are some sample inputs and outputs of the function `DrawCompanionShapes`. The original polygon $P$ is colored in blue, while the polygonal line that represents a potential $\hat{P}_\mu$ is colored in red.

- `DrawCompanionShapes[{1,I,-1,-I}]`

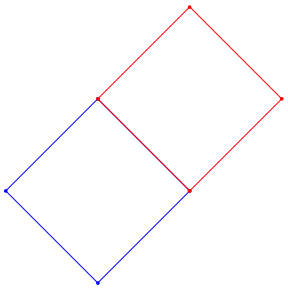

- `DrawCompanionShapes[{0,1,2+I,1+I}]`

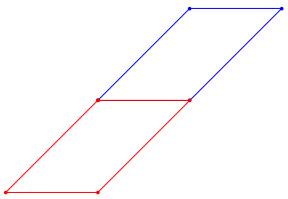

- `DrawCompanionShapes[{0,I,-1+I/2}]`

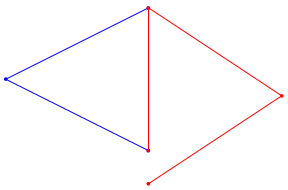

- `DrawCompanionShapes[{0,I,-1+I/2},{2Pi-2ArcTan[2],2Pi-2ArcTan[2],`
  `4ArcTan[2]}]`

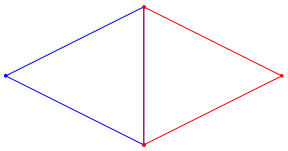

**7.2.6. Existence of $\hat{P}_\mu$.** As shown in the third example above, the polygonal line obtained from this algorithm may not form a closed polygon. In fact, the polygonal line is consisted of $n$ line segments with $n+1$ vertices. However, the desired polygon $\hat{P}_\mu$ should have exactly $n$ vertices corresponding to the number of vertices on $P$. In order to obtain $n$ vertices with the algorithm described above, the information we would need includes the side lengths $\ell_1, \ldots, \ell_{n-1}$, internal angles $\theta_2, \ldots, \theta_{n-1}$, and curvature data $\kappa(v_2), \ldots, \kappa(v_{n-1})$. Notice that the complete curvature data is not required to obtain $n$ vertices on the polygonal line, as we do not need the curvature information on two vertices $v_1$ and $v_n$. The $n+1$-st vertex $\hat{v}_{n+1}$ obtained from the algorithm allows us to determine whether the polygonal line can form a closed polygon, and it would consequently tell us whether the desired polygon $\hat{P}_\mu$ exists in our context. In the third example above, the uniform curvature distribution of $4\pi/3$ on each vertex does not produce a closed polygonal line, and thus the corresponding polygon $\hat{P}_\mu$ does not exist. However, in the fourth example with the same starting polygon $P$, a different curvature distribution yields a closed polygonal line, which realizes the polygon $\hat{P}_\mu$ as the triangle traced out in red. Details of the existence of $\hat{P}_\mu$ where $P$ is a polygon and $\mu$ is a discrete measure concentrated on the vertices of $P$ can be found in [**12**].

**7.2.7. Harmonic Cap Approximation.** We discussed in Chapter 2 that for a planar shape $P$ in $\mathbb{R}^2$ and its harmonic measure $\mu$ with respect to $\infty$ supported on $\partial P$, the harmonic cap $\hat{P}$ always exists. The `CompanionShape` function provides a discrete approximation to visualize the harmonic cap under specific circumstances.

Let $\Phi\colon \mathbb{C}\setminus\overline{\mathbb{D}} \to \mathbb{C}\setminus P$ be a conformal isomorphism that fixes the point at $\infty$. For $P$ with piecewise $C^1$ boundary, the map $\Phi$ extends continuously to the boundary $\partial\,\mathbb{D}$. Let $\{z_k\}_{k=1}^n$ be points uniformly distributed on $\partial\,\mathbb{D}$ with respect to arc length $\lambda$, *e.g.*, $z_k = e^{2k\pi i/n}$ the $n$-th roots of unity. As we pick $n$ big enough, the images $\Phi(z_k)$ forms a discrete approximation of $\partial P$ with respect to the harmonic measure $\mu = \Phi_*\lambda$. If the list $\{\Phi(z_k)\}_{k=1}^n$ is used as the vertex input for `CompanionShape` with curvature uniformly distributed on the sample vertices, a numerical approximation to the harmonic cap can be obtained. The resulting polygonal arc will have a very small (possibly zero) distance between the endpoints.

## 7.3. The Convex Body Associated to $W_{1/2}$

We have previously established

$$F_\theta(t) = f(\gamma(t)) = 2\theta^{-\theta/2}(2-\theta)^{\theta/2-1}\sin(t/2)^\theta\cos(t/2)^{2-\theta} \tag{1.3}$$

as the parametrization of $W_\theta \cap [0,1]$ with respect to conformal angle $t \in [0,\pi]$ in Theorem 1.4. We use this parametrization as the input to the cap construction algorithm.

**7.3.1. Constructing the Harmonic Cap.** The algorithm for the construction of the harmonic cap consists of the following steps.

(1) Choose a large positive integer $n$ that represents the number of discrete points to approximate the harmonic measure on *each* branch of the wedge $W_\theta$.

(2) Choose an integer $k$ such that $1 \le k \le n/2$. This is the number of discrete points that are supposed to approximate the harmonic measure on the inner side

of one branch of the wedge $W_\theta$. The integer $k$ determines the parameter $\theta$ by the relation

$$\arccos(1-\theta) = \frac{k\pi}{n}.$$

For example, $\theta = 1$ corresponds to $k = n/2$, where the wedge is a simple line segment, and $\theta = 1/2$ corresponds to $k = n/3$, where we have a right-angle wedge $W_{1/2}$.

(3) Use equation 1.3 to compute the image of $n$ equally spaced points

$$\exp\left(\frac{i\pi}{n}\right), \exp\left(\frac{2i\pi}{n}\right), \ldots, \exp\left(\frac{(n-1)i\pi}{n}\right), \exp(i\pi)$$

on the unit semicircular arc on the upper half plane joining 1 to $-1$. The distribution of these $n$ points provides a discrete approximation of the harmonic measure on one branch of the wedge $W_\theta$.

(4) Reflect the image obtained in the previous step to get a discrete approximation of the harmonic measure on the other branch of the wedge $W_\theta$. The joined list of $2n$ images provides a discrete parametrization of $W_\theta$ with respect to its harmonic measure. The parameterization traces (the outside of) the wedge $W_\theta$ twice in counterclockwise direction.

(5) Use the discrete approximation by $2n+1$ points obtained in the previous step as the input of `DrawCompanionShapes`, and get a sequence of $2n$ points on the boundary of the harmonic cap in the clockwise direction. The algorithm is relatively fast, as $n = 12000$ yields a result within 11 seconds, with computation precision in the order of $10^{-6}$.

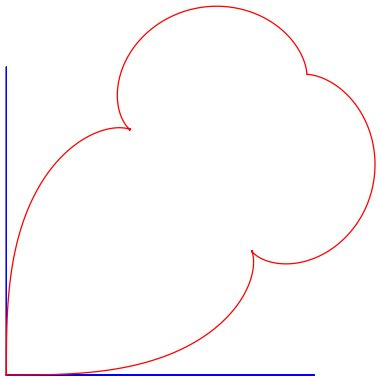

Figure 7.2. The right-angle wedge $W_{1/2}$ (blue) and its harmonic cap (red)

An image of $W_{1/2}$ together with its harmonic cap is generated with parameters $n = 12000$ and $k = 4000$. The first point of the harmonic cap, as well as the wedge, is set at 0, while the last point (the 24001-st) of the harmonic cap is at about $2.2 \times 10^{-6} - 2.2 \times 10^{-6} i$, whose distance to the origin is approximately $3.1 \times 10^{-6}$. Graphically, we are not be able to tell such small difference in the print-out of Figure 7.2.

**7.3.2. Folding the Petals.** In this subsection, we will use the figure of $W_{1/2}$ and its harmonic cap as an example.

The output of `DrawCompanionShapes` is a graphical object based on the computation result of `CompanionShape`, whose output is a list of $2n+1$ complex numbers, representing points on the boundary of the harmonic cap in clockwise direction. The following figure shows the locations of the first point, the $k+1$-st point, and the $n+1$-st point on the harmonic cap. We first establish the following guiding principles for folding up the harmonic cap to obtain the boundary surface of the associated convex body.

(1) No folding lines should cross in the interior of the harmonic cap.

(2) By symmetry, every folding line should have a mirror image, symmetric across the line joining the first point and the $n+1$-st point, that is also a folding line.

(3) The perimeter gluing shall identify the following two arcs together by arc length:

- The arc joining the $k+1$-st point to the first point;
- The arc joining the $k+1$-st point to the $n+1$-st point.

A few conclusions can be inferred from these principles.

(4) From principle (1) alone, if three folding lines form a triangle, then no other folding line should pass through the interior of this triangle, and thus the triangle is a planar face of the resulting convex body.

(5) From principles (1) and (2), we can infer that no folding line should cross the symmetry axis, unless it joins two points on the boundary symmetric across the axis.

(6) The gluing principle (3) indicates that there must be at least one folding line symmetric across the axis.

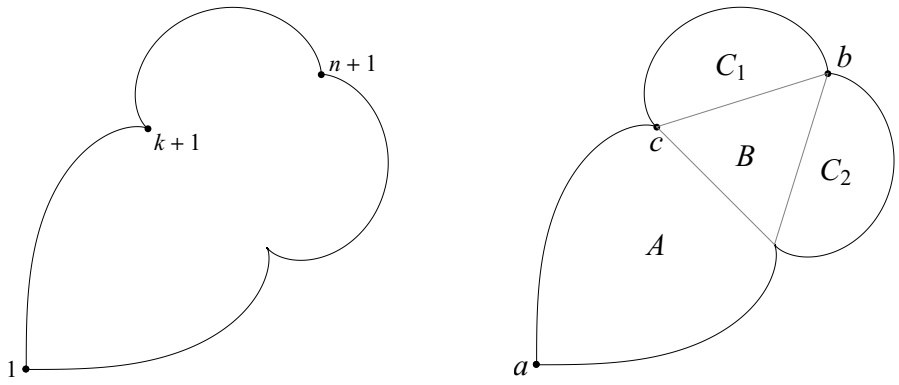


Figure 7.3. The harmonic cap of $W_{1/2}$, with $2n+1$ points approximating the boundary, partitioned into four regions

We first conjecture that the triangular region $B$ shown in Figure 7.3 is a planar face of the associated convex body.

It is easy to see that region $A$ is a curved face of the boundary surface of the associated convex body, as the regions $A$ and $B$ have different heights against their common base. We attempt to answer the question whether the regions $C_1$ and $C_2$ are planar faces of the convex body with the following strategy.

(1) Find an affine transformation $f(z) = e^{i\theta}z + \beta$ such that $f(b) = 0$ and $f(a) \in (-\infty, 0)$. The resulting image of the harmonic cap in the complex plane is shown in the figure below.

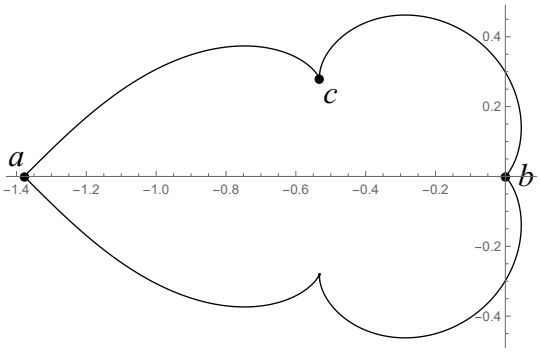


(2) Choose an assumed angle $\varphi$ of rotation. Isolate the boundary curve $\Gamma$ joining $b$ to $c$, and rotate along the line through $b$ and $c$ for $\varphi$ into the third dimension to

obtain $\Gamma_\varphi$.

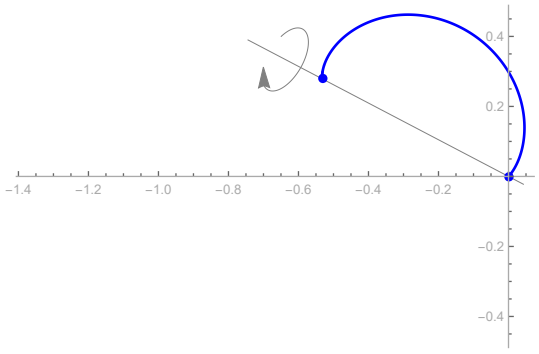


The results of the rotation for $\varphi = \pi/6$ and $\varphi = \pi/3$ are shown in the following figure.

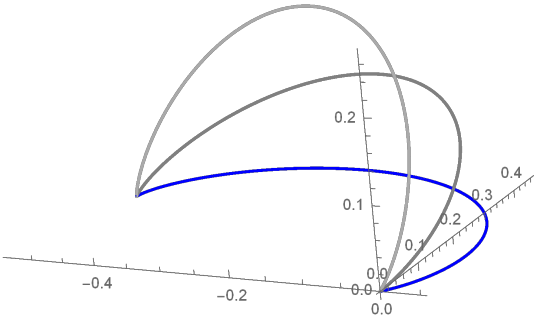


(3) Compute the curve in the plane that glues to the rotated image $\Gamma_\varphi$ to form half of a closed convex body. The algorithm includes the following steps.

- There are $n-k+1$ points on the curve $\Gamma_\varphi$. Isolate the $y$-coordinates of these points in a list `y`, and the projection onto the $xz$-plane in a list `xz`.
- Use the list `xz` to compute the `arclength` of the $xz$-projection of $\Gamma_\varphi$ starting from the point $f(c)$ in the complex plane.
- The list `arclength` contains the distance to the point $f(c)$ in the $x$-direction, and the list `y` contains the distance to the real axis in the $y$-direction. Hence, we obtain another list of $n-k+1$ points that forms the desired curve.

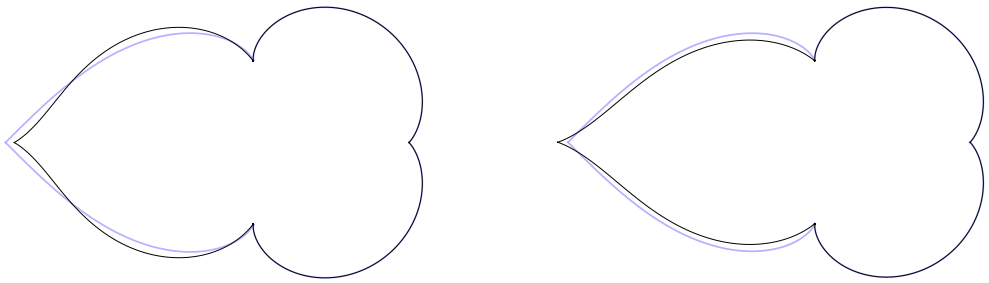

Figure 7.4. The caps of $W_{1/2}$, if the petals are assumed to be folded into planar faces, shown in thin black curves. The light blue curve shows the actual boundary of the harmonic cap of $W_{1/2}$.

Figure 7.4 shows two caps of $W_{1/2}$, if we assume that the petals $C_1$ and $C_2$ are planar faces of the associated convex body obtained from folding up the petals by $\varphi = \pi/4$ and $\varphi = \pi/3$, respectively. The images are superimposed with the actual *harmonic* cap of $W_{1/2}$ in light blue.

The images we obtained are strong evidence that the convex body associated with the harmonic cap has one and only one planar face, namely the region $B$.

**Proposition 7.1.** *The convex body associated with the harmonic cap of $W_\theta$ has the regions $C_1$ and $C_2$ as curved faces.*

Proof. Suppose that $C_1$ and $C_2$ are planar faces of the convex body. Then each of them forms a dihedral angle $\varphi$ with the planar face $B$. The sum of internal angles at the gluing site of the points $a$ and $b$ is therefore strictly less than $2\pi$. Hence, some amount of positive curvature is concentrated at a single point on the surface of the convex body, which would imply that the harmonic measure of $W_\theta$ is atomic at that point. Contradiction. □

## 7.4. The Zipper Algorithm

The zipper algorithm is an elementary algorithm for computing conformal maps discovered in the early 1980's by Kühnau and Marshall. Its convergence was studied by Marshall and Rohde [**14**]. We include a brief description of the algorithm itself, as many figures of harmonic caps in this thesis attributes to the zipper algorithm.

The elementary map of the zipper algorithm is the conformal map $f_a\colon \mathbb{H}\setminus\gamma_a \to \mathbb{H}$, where $\gamma_a$ is an arc of a hyperbolic geodesic from 0 to $a \in \mathbb{H}$. This map is realized by a composition of a Möbius transformation, the square, and the square root map.

Let

$$b = \frac{|a|^2}{\mathrm{Re}(a)} \text{ and } c = \frac{|a|^2}{\mathrm{Im}(a)}.$$

Then the geodesic arc $\gamma_a$ intersects $\mathbb{R}$ at $b$, and the Möbius transformation

$$z \mapsto \frac{z}{1 - z/b}$$

sends $\gamma_a$ to $\gamma_{ic}$, which is a line segment orthogonal to $\mathbb{R}$ from 0 to $ic$. Compose this map with $z \mapsto z^2 + c^2$ and then $\sqrt{z}$, we obtain the desired conformal map $f_a$ as shown in Figure 7.5.

The inverse $f_a^{-1}$ can be easily found by composing the inverses of these elementary functions in the reverse order.

Let $z_0, z_1, \ldots, z_n$ be points on the boundary of a Jordan domain $\Omega$ traced in the counter-clockwise direction. The map $\varphi_1$ given by

$$\varphi_1(z) = i\sqrt{\frac{z - z_1}{z - z_0}}$$

maps $z_0 \mapsto \infty$, $z_1 \mapsto 0$, and all other $z_i \mapsto \varphi_1(z_i) \in \mathbb{H}$. The interior of $\Omega$ is mapped to the "left" of 0, and the exterior of $\Omega$ is mapped to the "right" of 0 on $\mathbb{H}$.

Now we set $\zeta_2 = \varphi_1(z_2)$ and $\varphi_2 = f_{\zeta_2}$. Repeating this process, and define

$$\zeta_k = \varphi_{k-1} \circ \cdots \circ \varphi_1(z_k), \text{ and } \varphi_k = f_{\zeta_k}.$$

Here we just use the elementary conformal map to "unzip" the boundary of the Jordan domain onto the positive and negative real axis. Notice that each elementary conformal map maps $\mathbb{R}$ into (but not onto) $\mathbb{R}$. Finally, map a half-disk to $\mathbb{H}$ by letting

$$\zeta_{n+1} = \varphi_n \circ \cdots \circ \varphi_1(z_0) \in \mathbb{R},$$

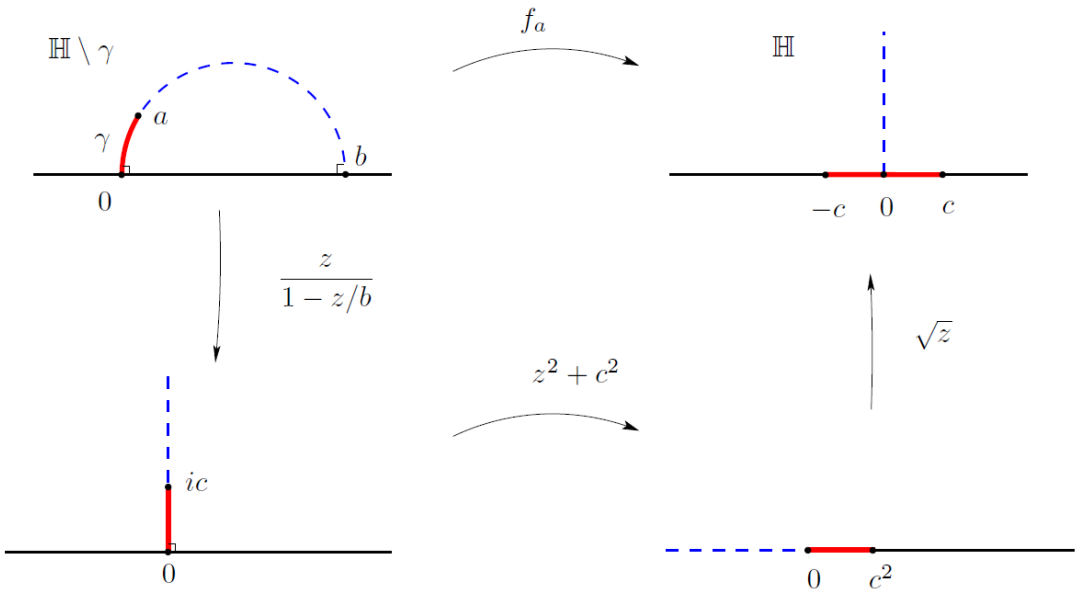


Figure 7.5. The elementary map of the zipper algorithm, figure excerpted from [**14**]

and set

$$\varphi_{n+1} = \left(\frac{\zeta_{n+1} - z}{z}\right)^2.$$

Let

$$\varphi = \varphi_{n+1} \circ \varphi_n \circ \cdots \circ \varphi_2 \circ \varphi_1, \text{ and } \varphi^{-1} = \varphi_1^{-1} \circ \varphi_2^{-1} \circ \cdots \circ \varphi_n^{-1} \circ \varphi_{n+1}^{-1}.$$

Then $\varphi^{-1}\colon \mathbb{H} \to \Omega_c$ is a conformal isomorphism such that $z_j \in \partial\Omega_c$, and the portion $\gamma_j$ of $\partial\Omega_c$ connecting $z_j$ and $z_{j+1}$ is the image of the corresponding geodesic arc $\gamma_{\zeta_{j+1}}$ by the analytic map $\varphi_1^{-1} \circ \cdots \circ \varphi_j^{-1}$.

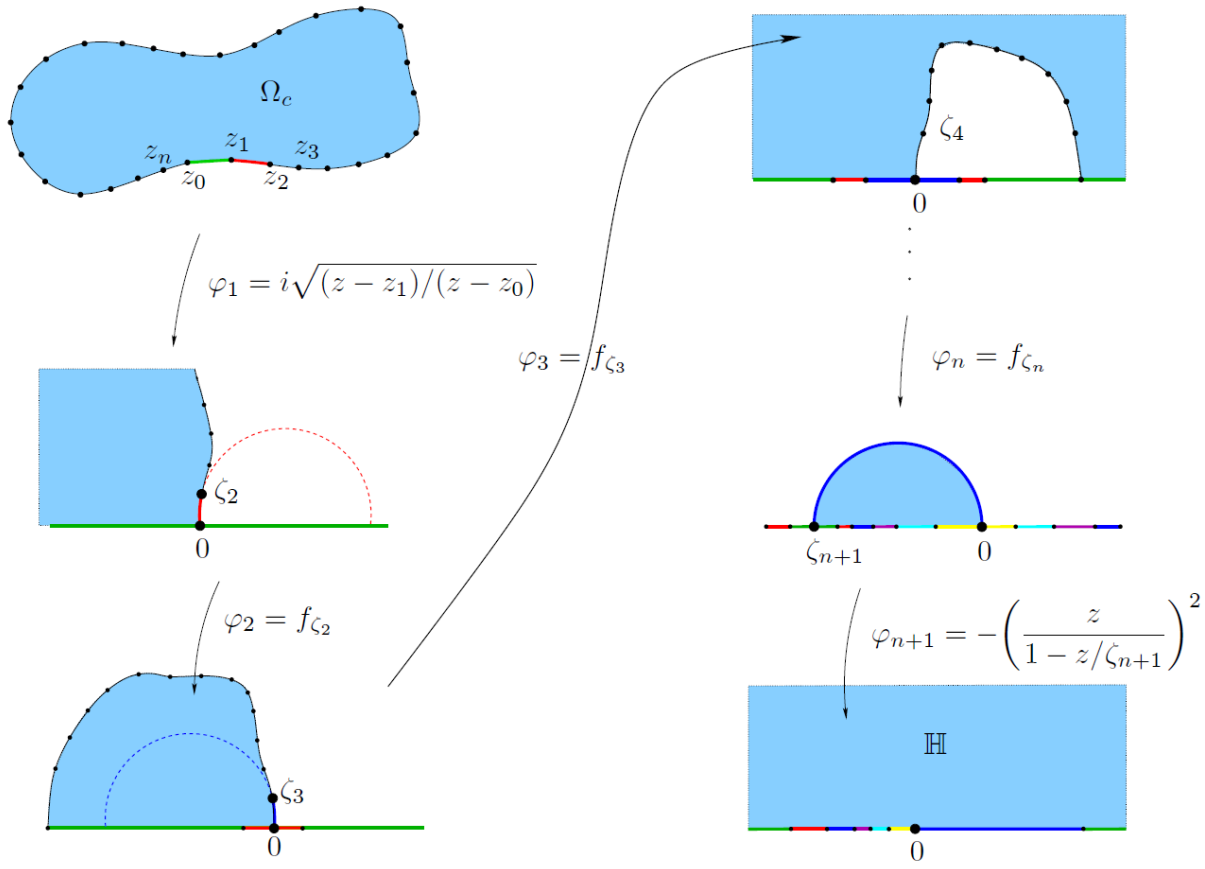


Figure 7.6. The zipper algorithm, figure excerpted from [**14**]

**Remark 7.2.** As remarked above, $\partial\Omega_c$ is piecewise analytic. In fact, it is also $C^1$ since the inverse of $f_a$ doubles angle at 0 and halves angles at $\pm c$.

**Remark 7.3.** The map $\varphi$ constructed above is also a conformal map of the complement of $\Omega_c$ onto the lower half plane.

CHAPTER 8

# Iterated Harmonic Caps and Plane Curves

## 8.1. Iterated Harmonic Caps

An observation that arises from the harmonic cap study is that the iterative process of taking harmonic caps appears to produce "rounder and rounder" planar shapes. This phenomenon is best illustrated in the sequence of the iterative images of the square under the operation of "taking harmonic cap". The sixth iteration has the same circumference as the initial square, but it is close, in the Hausdorff sense, to the round disk with the same circumference. With a lot of experimentations on the cap construction algorithm, we observe that this phenomenon is not limited to convex regions with symmetry such as a square. Included are the iterative images of a "keyhole" shape and an "L" shape under the same operation.

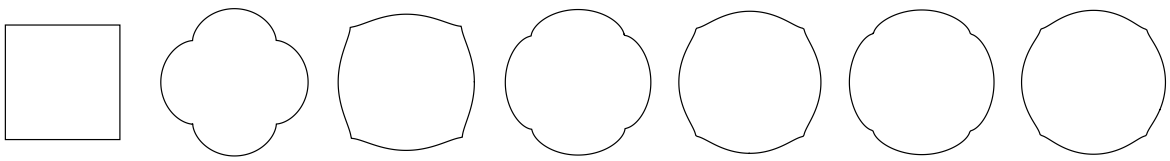

Figure 8.1. Iterative harmonic caps of the square

As we mentioned briefly in Chapter 3, the development of a harmonic cap may not be globally one-to-one, which prohibits the iteration process. We restrict the iteration process to Jordan domains whose iterative harmonic caps are all bounded by Jordan curves. The following conjecture describes our observation above.

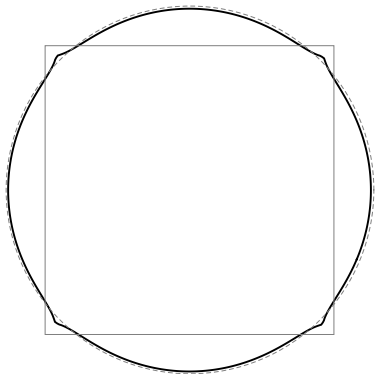

Figure 8.2. The sixth iterative harmonic cap of the square is close to a round disk (dashed curve) in the Hausdorff sense.

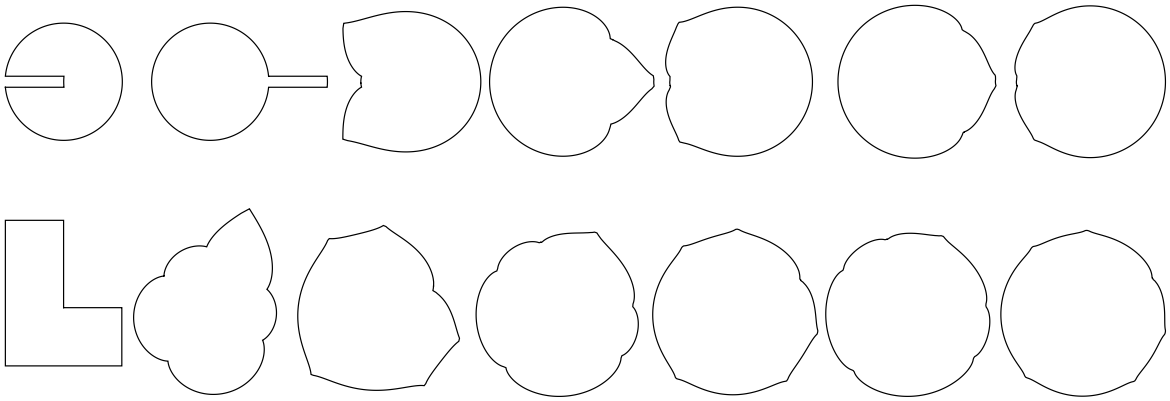

Figure 8.3. Iterative harmonic caps of the "keyhole" and the "L". The image of the first iteration of the "keyhole" was produced by the heuristic that as the keyhole gets sufficiently thin, the harmonic measure will concentrate so little within the keyhole that the harmonic cap simply recreate the shape of the keyhole outside of the disk region.

**Conjecture.** *Let $L > 0$. Let $\mathcal{R}(L)$ be the collection of rectifiable closed curves of length $L$, and let $\mathcal{J}(L) \subseteq \mathcal{R}(L)$ be the Jordan curves among them. Let $h\colon \mathcal{J}(L) \to \mathcal{R}(L)$ be the function that maps a Jordan curve $\Gamma \in \mathcal{J}(L)$ to the boundary curve of the harmonic*

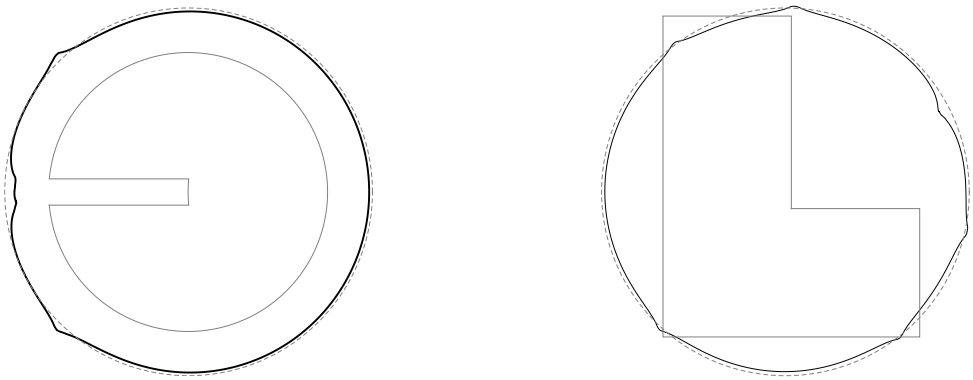

Figure 8.4. The sixth iterative harmonic caps of the "keyhole" and the "L" are close to round disks (dashed curves) in the Hausdorff sense.

*cap of the region bounded by* $\Gamma$. *Equation 3.2 guarantees that* $h$ *is well-defined. Let*

$$\mathcal{H}(L) = \bigcap_{n \geq 0} h^{-n}(\mathcal{J}(L)).$$

*Then the restriction* $h\colon\ \mathcal{H}(L) \to \mathcal{H}(L)$ *is also well-defined. If* $\Gamma \in \mathcal{H}(L)$, *then the sequence of Jordan curves* $\{h^n(\Gamma)\}_{n \geq 0}$ *converges to the circle* $C_L$ *of circumference* $L$ *in the Hausdorff metric.*

### 8.2. Plane Curve Iteration with the Symmetry Assumption

At the end of Chapter 5, we presented two ways to recover a Jordan arc from the conformal isomorphism $\Phi$, through the complement of the image and through the symmetry assumption. We concluded that the collection of all harmonically planar Jordan arcs is all curves with agreeing recovery from both methods. To find out whether a smooth Jordan arc $\Gamma$ is harmonically planar, it is then natural to take the following steps:

(1) Find an arc-length parameterization $\gamma\colon [0, L] \to \mathbb{C}$ of $\Gamma$. Translate and rotate $\Gamma$ such that $\gamma(0) = 0$ and $\gamma'(0) = 1$.

(2) Compute the conformal isomorphism $\Phi\colon\ \hat{\mathbb{C}}\setminus\overline{\mathbb{D}} \to \hat{\mathbb{C}}\setminus\Gamma$ that satisfies $\Phi(\infty) = \infty$ and $\Phi(1) = 0$.

(3) Find continuous functions $\varphi, \psi\colon [0, L] \to \partial\,\mathbb{D}$ such that $\Phi(\varphi(t)) = \Phi(\psi(t)) = \gamma(t)$.

(4) Construct a new curve $\tilde{\Gamma}$ by

$$\tilde{\gamma}(t) = \int_0^t \varphi(x)\psi(x)\,dx.$$

(5) $\Gamma$ is harmonically planar if and only if $\Gamma$ and $\tilde{\Gamma}$ are the same curve, or equivalently, if $\gamma'(t) = \tilde{\gamma}'(t)$.

Steps (1)–(4) describes a map that takes in a smooth Jordan arc $\Gamma$, and gives another curve $\tilde{\Gamma}$. This potentially defines an iterative process as well, if we assume that every iterative image is also a Jordan arc. We expect the fixed points of this iterative process to be the harmonically planar smooth Jordan arcs.

From the discussion in Section 6.3, we know that $W_\theta$ is not harmonically planar. Figure 8.5 shows the first five iterative images of three wedges with different incident angles. These examples appears to have their iterative images converging to circular arcs, which we know by Theorem 1.2 are harmonically planar. More examples are needed before we can propose a conjecture similar with the one on harmonic cap iteration.

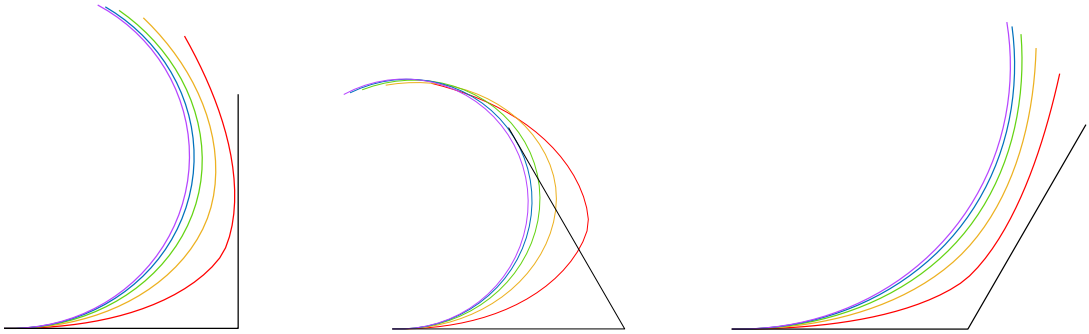

Figure 8.5. Iterative curves of the wedge family. The original curve is shown in black, and the following successive images are shown in red, yellow, green, blue, and purple, respectively. Each curve is a numerical approximation by a polygonal line of 40 segments.

# References


[1] Alexandrov, A. *Convex Polyhedra*. Springer Monographs in Mathematics. Springer Berlin Heidelberg, 2006.

[2] Beckenbach, E. F. The stronger form of Cauchy's integral theorem. *Bull. Amer. Math. Soc. 49*, 8 (08 1943), 615–618.

[3] Binder, I., Rojas, C., and Yampolsky, M. Carathéodory convergence and harmonic measure. *Potential Analysis 51* (2019), 499–509.

[4] Bobenko, A. I., and Izmestiev, I. Alexandrov's theorem, weighted delaunay triangulations, and mixed volumes. *Annales de l'Institut Fourier 58*, 2 (2008), 447–505.

[5] Demaine, E. D., and O'Rourke, J. *Geometric Folding Algorithms: Linkages, Origami, Polyhedra*. Cambridge University Press, 2007.

[6] DeMarco, L., and Lindsey, K. Convex shapes and harmonic caps. *Arnold Mathematical Journal 3*, 1 (Apr 2017), 97–117.

[7] Driscoll, T. A. The Schwarz-Christoffel toolbox for MATLAB. `http://www.math.udel.edu/~driscoll/SC/`. [online; accessed October 25, 2019].

[8] Driscoll, T. A. Algorithm 756: A MATLAB toolbox for Schwarz-Christoffel mapping. *ACM Trans. Math. Softw. 22*, 2 (June 1996), 168–186.

[9] Driscoll, T. A., and Trefethen, L. N. *Schwarz-Christoffel Mapping*. Cambridge Monographs on Applied and Computational Mathematics. Cambridge University Press, 2002.

[10] Duren, P. *Univalent Functions*. Grundlehren der mathematischen Wissenschaften in Einzeldarstellungen. Springer-Verlag, 1983.

[11] Garnett, J. B., and Marshall, D. E. *Harmonic Measure*. New Mathematical Monographs. Cambridge University Press, 2005.

[12] Han, Y., and Weng, S. Companion shapes and their Alexandrov realization. preprint available on webpage at `https://sites.math.northwestern.edu/~sweng/`, 2020.

[13] Marshall, D. E. Numerical conformal mapping software: Zipper. `https://sites.math.washington.edu/~marshall/zipper.html`, 2010. [online; accessed October 25, 2019].

[14] Marshall, D. E., and Rohde, S. Convergence of a variant of the zipper algorithm for conformal mapping. *SIAM Journal on Numerical Analysis 45*, 6 (2007), 2577–2609.

[15] Mörters, P., and Peres, Y. *Brownian Motion*. Cambridge Series in Statistical and Probabilistic Mathematics. Cambridge University Press, 2010.

[16] O'Rourke, J. On Flat Polyhedra deriving from Alexandrov's Theorem. *arXiv e-prints* (July 2010), arXiv:1007.2016.

[17] Ransford, T. *Potential Theory in the Complex Plane*. London Mathematical Society Student Texts. Cambridge University Press, 1995.

[18] Reshetnyak, Y. G. *Two-Dimensional Manifolds of Bounded Curvature*. Springer Berlin Heidelberg, Berlin, Heidelberg, 1993, pp. 3–163.

[19] Stephenson, K. Circle packing: a mathematical tale. *Notices Amer. Math. Soc 50* (2003), 1376–1388.

[20] Sullivan, J. M. Curvatures of smooth and discrete surfaces, 2007.

[21] Toponogov, V. A. *Differential geometry of curves and surfaces*. Springer, 2006.

# Vita

The author grew up in Nanjing, China. He received a Bachelor of Arts in Mathematics and Chemistry at Bard College in 2015. Later that year, he enrolled in the Ph.D. program in mathematics at Northwestern University. He will complete his Ph.D. in the summer of 2020.